Journal of Catalysis 385 (2020) 160–175

Contents lists available at ScienceDirect

Journal of Catalysis

journal homepage: www.elsevier.com/locate/jcat

Continuous catalytic process for the selective dehydration of glycerol over Cu-based mixed oxide

Jaime Mazarío, Patricia Concepción, María Ventura, Marcelo E. Domine *

Instituto de Tecnología Química (UPV-CSIC), Universitat Politècnica de València, Consejo Superior de Investigaciones Científicas, Avda. de los Naranjos s/n, 46022 Valencia, Spain

ARTICLE INFO

Article history:
Received 9 September 2019
Revised 9 March 2020
Accepted 15 March 2020

Keywords:
Acetol
Glycerol
Glycerol dehydration
Copper catalyst
Mixed oxides

ABSTRACT

The selective dehydration of glycerol to hydroxyacetone (acetol) was studied with Cu-based mixed oxides derived from hydrotalcite as catalysts in a continuous flow fix-bed reactor. Catalysts were prepared by co-precipitation and characterized by ICP, N_2 adsorption, XRD, NH_3-TPD, CO_2-TPD, TPR and TEM. Different parameters were investigated to develop the most appropriate material as well as to determine the function of every metallic species. The optimized Cu-Mg-AlO_x offered ≈60% acetol selectivity at >90% glycerol conversion (≈80% liquid yield, up to TOS = 9 h). The catalyst could be regenerated by calcination, achieving full activity recovery after five re-cycles. "In-situ" FTIR and XPS measurements evidenced that the presence of Cu, specially the most active Cu^{1+} species, was essential to carry out the dehydration to acetol with high reaction rates, and to form the preferred intermediate (with C=O group); although a minor contribution from Cu^0 and Cu^{2+} species could not be discarded.

1. Introduction

Nowadays, fossil fuels such as coal, petroleum and natural gas provide more than 75% of the total energy consumed in our planet and represent an essential source of raw materials for the chemical industry [1]. Nonetheless, the growing use of these resources has led to their depletion along with an increment in the levels of CO_2 emissions to the atmosphere, which is considered as the main cause of the greenhouse gases (GHG) effect in the planet. Thus, the conversion of alternative, clean and renewable raw materials such as biomass into fuels and chemicals has become an interesting way of dealing with global warming and contributing to the diversity of energy sources [2–5].

In the last years, a wide variety of the so-called biofuels has appeared in the market: bioethanol, biobutanol, biodiesel, biogas or pyrolysis gases as promising renewable alternatives [6]. The common feature of these biofuels is the reduced amount of greenhouse gases generated while using them in different applications, thereby allowing to design processes without CO_2 net emission provided that efficient crop methods are developed to produce the biomass of interest [3,5].

Regarding the biodiesel, it is synthesized by means of a transesterification reaction using triglycerides (vegetable oils) and methanol or ethanol to produce the corresponding methyl or ethyl-esters. The raw materials being the source of triglycerides used to be colza, sunflower, soy or palm oil, whereas the biodiesel obtained can be used directly as a fuel or mixed with petrodiesel in different ratios [3]. However, in the last years, and due to the constrains derived from the use of agricultural suitable land and vegetables for fuel industry against food applications, biodiesel production coming from the transformation and upgrading of used oils derived from food industry, as well as from other residues and unconventional raw materials (i.e. animal fats, agricultural and domestic wastes, oil wastes, etc.) [7–9] started to be developed. Even in these novel cases, huge amounts of glycerol are also obtained as a by-product, which is supposed to be somehow used if the biorefinery wants the process to be profitable [10]. Consequently, the transformation and valorization of glycerol has been broadly studied by many research groups working in catalysis, and compiled in some interesting reviews [11–13]. This academic effort has resulted in glycerol integrating the list of the twelve more important platform molecules derived from biomass [14]. Many possibilities of valorization for this molecule by using heterogenous catalysis have been developed in the last years. Processes such as the synthesis of glycerol carbonate for solvent and polymer production with hydrotalcite-derived oxides [15] or zeolites [16] as catalysts, the glycerol steam reforming to produce *syn*-gas using catalysts containing Pt, Ru or Re supported on different inorganic matrix [17], as well as the manufacture of fuel additives by means of glycerol acetalization, etherification or

* Corresponding author.
E-mail address: mdomine@itq.upv.es (M.E. Domine).

https://doi.org/10.1016/j.jcat.2020.03.010
0021-9517/

esterification reactions [18] are among the most relevant catalytic strategies up to now reported.

The selective dehydration of glycerol to hydroxyacetone (or acetol) is of interest if the reactivity of this molecule, having a terminal hydroxyl group and a carbonyl group in the second carbon, is considered. These functional features give this molecule the possibility of taking part in different organic reactions such as the Mannich reaction [19] or some aldolic condensations [20]. Besides, acetol is a key intermediate in the production of 1,2-propanediol or propylene glycol [21]. Therefore, a better understanding of this glycerol dehydration could also give an improvement on the yield to propylene glycol and on any product derived from it.

With respect to acetol production, Chiu et al. have studied the dehydration of glycerol to acetol with different heterogeneous catalysts in a reactive distillation system, the highest values of conversion and selectivity being reached with copper-chromite catalyst [22]. Nevertheless, copper-chromite cannot be considered as an environmentally friendly catalyst due to its toxicity and, additionally, the scale-up of a reactive distillation system is not straightforward from an industrial viewpoint. In this sense, continuous catalytic processes would be more suitable, although just a few articles can be found in the literature [23–25], most of them involving the use of hydrogen. In this regard, it would be very interesting to develop a continuous and sustainable process for the selective dehydration of glycerol to acetol by using an efficient heterogeneous catalyst.

Due to the considerable number of studies carried out to produce acrolein, the other possible dehydration product from glycerol, Brönsted acid centers are believed to present a higher selectivity to its formation. On the contrary, Lewis acid centers would in principle provide more selectivity towards acetol [26,27]. Nonetheless, it is worth noting that some contradictory opinions can be found in the literature about the reaction mechanism of this system. Some authors argue that the acetol formation could be favored by a certain ratio between acid and basic Lewis centers [28,29]. Following this idea, and to effectively carry out the selective dehydration of glycerol to acetol, it is reasonable to think that the combination of both acid and basic Lewis centers contained in metallic mixed oxides derived from hydrotalcites constitutes an excellent alternative to accomplish this target.

Hydrotalcite-type materials are Mg-Al lamellar double hydroxides with a structure derived from brucite [$Mg(OH)_2$]. This structure is constituted by two dioctahedral sheets of magnesium hydroxide with water molecules in the interlaminar space. Hydrotalcites are the result of an isomorphic substitution of some Mg^{2+} by Al^{3+} thereby the sheet acquires a positive charge which allows several anions to be located beside the water molecules in the interlaminar space (in its natural state mainly OH^- and CO_3^{2-}). This structure is common to many natural and synthetic materials having the same empirical formula [30–32]: $M_a^{2+}M_b^{3+}(OH)_{2a+2b}(X^-)_{2b}\cdot xH_2O$. During the calcination, the structure collapses and yields a low-crystalline mixed oxide with cationic vacancies produced due to the need of equilibrating the excess of positive charge introduced by replacing some Mg^{2+} by Al^{3+}. Therefore, with respect to MgO, the material exhibits some stronger Lewis basic sites, corresponding to unsaturated O^{2-}, and some weak acid sites, corresponding to Al^{3+} [32–34].

Among their many advantages, hydrotalcite-type materials have an easy and low-cost synthesis procedure; they are non-toxic and possess the capacity of easily modifying their physicochemical properties by means of controlling their composition. Thus, amount and strength of both basic and acid sites can be adapted to the catalytic process needs just by changing the M^{2+}/M^{3+} molar ratio. In addition, different metals (others than Mg and Al) can also be incorporated in the hydrotalcite precursor either during the synthesis or in post-synthesis steps, thus extending the versatility of these materials.

In light of all the above-mentioned, in this work an efficient continuous catalytic process for the selective dehydration of glycerol to acetol (see Scheme 1) in a fixed bed reactor by using transition metal hydrotalcite-derived materials as catalysts and without introducing hydrogen in the reactor is designed and optimized. Concretely, Mg/Al hydrotalcite-type materials with different amounts of Cu, Ni, or Co were prepared, since these transition metals have been reported to help to produce acetol as an intermediate during glycerol reforming [35,36]. Their hydrotalcite-derived metallic mixed oxides were evaluated in the production of the desired acetol from glycerol. Special attention is paid to the role of copper in the formation of acetol and the influence of its oxidation state in that process, as it appears to be a key point to generate the dehydration product, as it was observed during glycerol hydrogenolysis process [37,38].

2. Experimental

2.1. Materials

Glycerol (Sigma-Aldrich, 99.5%) was used as reagent in the dehydration reaction. For the analysis of the reaction products acetol (90%), methyl glycolate (99%), methyl lactate (98%), acetoin (98%), methyl pyruvate (98%), acetic acid (99%), propionic acid (99.5%), 1,2-propanediol 99.5%), 1,3-propanediol (98%), methyl acetate (98%), methyl formiate (99%) and chlorobenzene (internal standard, 99%) were purchased from Sigma-Aldrich and used as received. Acrolein (Merck, 95%) and dihydroxyacetone (Merck, 98%) were also used. Methanol (reagent grade 99.9%) supplied by Scharlau and water (Milli-Q quality, Millipore) were used as solvents. Hydrotalcite-type materials were prepared by using in each case the suitable metallic precursors bought from Sigma-Aldrich: $Mg(NO_3)_2\cdot 6H_2O$ (99%), $Al(NO_3)_3\cdot 9H_2O$ (98%), $Cu(NO_3)_2\cdot 2.5H_2O$ (98%), $Ni(NO_3)_2\cdot 6H_2O$ (98.5%) and $Co(NO_3)_2\cdot 6H_2O$ (98%). In addition, Na_2CO_3 (Fisher Chemical, 99.7%), NaOH (Sigma-Aldrich, 98.0%) and H_2O (milliQ, Millipore) were also used for their synthesis. For comparative purposes MgO and Al_2O_3 (Sigma-Aldrich) were also tested in the reaction. Hydrogen (99.999%) was purchased from Abelló Linde S.A.

2.2. Catalyst preparation

Hydrotalcite-type materials were prepared by the co-precipitation method under well optimized synthesis (and aging) conditions, following the procedure described in refs. [15,39] and starting from two different solutions. Solution A, containing the metallic species (Al, Mg and Cu/Ni/Co) in the desired molar ratios as nitrates and not exceeding 1.5 of total cationic concentration; and solution B, containing sodium hydroxide and sodium carbonate in adequate amounts to accomplish a CO_3^{2-}/(total cationic number) ratio always equal to 0.66. These solutions were added at the same rate (20 mL/h) to an empty plastic beaker with continuous stirring at 200 rpm. The precipitates were aged at 60 °C overnight in a thermostatic bath. The resulting products were filtered and washed thoroughly with deionized water until pH = 7. Depending on the transition metal to be incorporated in the hydrotalcite, the

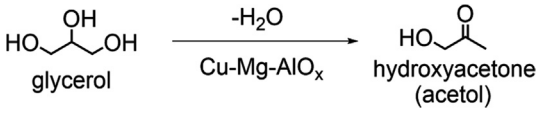

Scheme 1. Selective dehydration of glycerol to acetol over Cu-Mg-Al mixed oxide.

corresponding Cu [$Cu(NO_3)_2{\cdot}2.5H_2O$], Ni [$Ni(NO_3)_2{\cdot}6H_2O$] or Co [$Co(NO_3)_2{\cdot}6H_2O$] precursors were used. The hydrotalcites were calcined at 550 °C during 6 h in air to yield the corresponding metal-based mixed oxides used in the catalytic tests. Additionally, and in the case of Cu-based samples, one material was reduced under H_2 flow (100 mL/min) at 450 °C during 3 h, and another amount of the same material was partially reduced at 200 °C during 3 h, prior to their use in the catalytic experiments.

2.3. Catalyst characterization

Hydrotalcite-type and metal mixed oxides materials were characterized by ICP (inductively coupled plasma), with a Varian 715-ES ICP-Optical Emission spectrometer, after solid dissolution in HNO_3/HCl aqueous solution. Phase purity of the catalysts was determined by X-ray diffraction (XRD) in a Philips X'Pert MPD diffractometer equipped with a PW3050 goniometer (CuK_α radiation, graphite monochromator), provided with a variable divergence slit and working in the fixed irradiated area mode. The obtained diffractograms were compared with those found at the PDF2 database (codes in parenthesis). Surface areas of the solid samples (200 mg) were calculated by applying the BET method to the N_2 adsorption isotherms obtained by carrying out liquid nitrogen adsorption experiments at 77 K, in a Micromeritics flowsorb apparatus.

The reduction behavior of copper in these materials was studied by temperature-programmed reduction (TPR) analysis carried out in a Micromeritics Autochem 2910 equipment. About 30 mg of sample were initially flushed with 30 cm^3/min of Ar at room temperature for 30 min, and then a mixture of 10 vol% of H_2 in Ar was passed through the catalyst at a total flow rate of 50 cm^3/min, while the temperature was increased up to 1273 K at a heating rate of 10 K/min. The H_2 consumption rate was monitored in a thermal conductivity detector (TCD) previously calibrated using the reduction of CuO as reference. In addition, X-ray photoelectron spectroscopy (XPS) was used to determine the oxidation states of copper species at the catalyst surface. XPS data were collected on a SPECS spectrometer equipped with a 150-MCD-9 detector and using a non-monochromatic Mg Kα (1253.6 eV) X-ray source. Spectra were recorded at 25 °C, using an analyzer pass energy of 30 eV, an X-ray power of 50 W (to avoid photo-reduction) and under an operating pressure of 10^{-9} mbar. During data processing of the XPS spectra, binding energy (BE) values were referenced to the Al 2p peak settled at 73.5 eV. Spectra treatment was performed using the CASA software.

Acid and basic centers present in our materials were determined by temperature programmed desorption of ammonia (NH_3-TPD) and carbon dioxide (CO_2-TPD), respectively, carried out on a TPD/2900 apparatus from Micromeritics. Approximately, 0.100 g of sample were pre-treated in an Ar stream at 300 °C during 1 h. Ammonia was chemisorbed by pulses at 100 °C until equilibrium was reached, while carbon dioxide was chemisorbed in the same way at room temperature. Then, the sample was fluxed with helium stream during 15 min, prior to increase the temperature up to either 500 °C (NH_3) or 650 °C (CO_2) in a helium stream of 100 mL/min and using a heating rate of 10 °C/min. Gas adsorption was monitored with a calibrated thermal conductivity detector (TCD), representing a quantitative value. On the other hand, a non-calibrated mass-spectrometer (MS) was used to follow ammonia desorption, providing us with a qualitative information about the strength distribution of acid sites.

FT-IR spectrometry studies were recorded with a Bruker 70 V spectrometer using a DTGS detector and acquiring at 4 cm^{-1} resolution. An IR cell allowing *"in situ"* treatments in controlled atmospheres and temperatures from 25 °C to 500 °C was connected to a vacuum system with gas/liquid dosing facility. For IR studies the samples were pressed into self-supported wafers and treated at 300 °C in Nitrogen flow (20 mL·min^{-1}) during 1 h followed by evacuation at 10^{-4} mbar at 100 °C during 1 h, except in the ex situ H_2 reduced sample which was activated in vacuum at 100 °C for 1 h. After activation the samples were cooled down to 25 °C under dynamic vacuum conditions and exposed to 1.5 mbar of 1,2-propanediol and/or hydroxyacetone followed by evacuation at 25 °C during 5 min. In the case of 1,2-propanediol the temperature was risen under static vacuum conditions to 80 °C and 160 °C acquiring IR spectra at 45 min of each temperature. Once achieved 45 min at 160 °C, the sample was evacuated and cooled down to 25 °C where 10 mbar CO has been adsorbed for surface titration. In order to avoid surface reduction by CO, IR spectra was immediately collected. IR spectra were processed using the Origin software. For NO adsorption studies, after activation the samples were cooled down to −156 °C under dynamic vacuum conditions followed by NO dosing at increasing pressure (0.05–0.60 mbar). IR spectra were recorded after each dosage. After maximum NO dosing, the samples were evacuated under dynamic vacuum conditions at 10^{-5} mbar and IR spectra acquired at controlled times.

High-resolution transmission electron microscopy (HR-TEM) was done using a Jeol JEM-2100F operating at 200 kV. The microscope was also equipped with a high-angle annular dark-field (HAADF) detector and an EDS X-Max 80 detector. HR micrograph analysis, lattice spacing, First Fourier Transform (FFT) and phase interpretation, were done with the Gatan Digital Micrograph software (Gatan Inc.). Besides, thanks to the EDS detector, with a resolution of 127 eV, maps with different colours depending on the element were obtained. Jeol JSM6300 operating at 20 kV and equipped with an energy-dispersive X-ray spectrometer (EDX) was used to obtain Screen Electron Microscopy (SEM) images and compositional mappings.

Thermogravimetric analyses (TG) were carried out in a Mettler Toledo TGA/SDTA 851 apparatus, using a heating rate of 10 °C/min in an air stream until 800 °C was reached. Elemental analysis (EA) was carried out in a Fisons EA1108CHN-S apparatus. These two techniques (TG and EA) together with ICP, N_2 adsorption and XRD measurements were applied to determine and evaluate the organic content, the metal leaching, and the stability of metal mixed oxide structures, respectively, after several consecutive uses of the catalysts under reaction conditions.

2.4. Catalytic tests

Catalytic experiments were performed in a stainless-steel tubular fixed-bed reactor (length = 25 cm and diameter = 0.5 cm), with the catalyst pelletized in particles 0.4–0.6 mm in size and diluted with SiC (0.6–0.8 mm). Typically, catalytic tests were carried out by feeding the reactor with a liquid mixture of glycerol (GLY) and methanol (MeOH) (10:90 wt ratio) at temperatures between 220 and 280 °C during 9 h. For each experiment, cumulative fractions corresponding to 0–1 h, 1–2 h, 2–3 h, etc. were collected in a glass recipient submerged in an ice bath, and then analyzed by HPLC (Shimadzu Nexera LC-20 AD XR, reverse phase, Hi-Plex H Column 300 × 7.7 mm, and PL Hi-Plex Guard Column 50 × 7.7 m m), and also by GC (Varian CP-3800, CARBOWAX Column 15 m × 3.2 mm). Product identification was done by GC–MS (Agilent 6890N GC System coupled with an Agilent 5973N mass detector).

With the aim of calculating conversions and, taking into account that some few amounts of glycerol are retained on the catalytic surface and part of it could be later transformed into coke, the total yield to products was considered as the actual conversion, as it gives more information about the "effective activity" of our materials:

$$X_{glycerol}(\%) = \frac{\sum n^{f}_{product_i} a_i}{n^{0}_{glycerol}} \cdot 100 \quad (1)$$

Being a_i the stoichiometric correction factor for the product$_i$.

Selectivity to acetol (and to the different products) was also calculated as a function of the total amount of products as follows:

$$S_{acetol}(\%) = \frac{n^{f}_{acetol}}{n^{f}_{total\ products}} \cdot 100 \quad (2)$$

Finally, gaseous products mainly derived from methanol conversion in some specific pre-treatment experiments were analyzed at the exit of the reactor. The gas composition was determined using a GC fitted with 3 detection lines: (i) one for H_2 separated on a 5A molecular sieve column (with Ar as carrier) and quantified on a TCD, (ii) a second one for N_2 separated on a 13X molecular sieve column (with He as carrier) and quantified on a second TCD, and iii) a third one equipped with Al-plot column (with He as carrier) and a FID detector for hydrocarbons quantification. This, together, with the TG analysis (see Section 2.3) allowed us to calculate the carbon balance of the reaction with respect to the total amount of glycerol fed into the reactor.

$$CB_{glycerol}(\%) = \frac{\sum n^{f}_{product_i} \cdot x_i C\ \ atoms}{n^{0}_{glycerol} \cdot 3C\ \ atoms} \cdot 100 \quad (3)$$

Being x_i the number of carbon atoms in the *product*$_i$ coming from glycerol reaction.

2.5. Re-usability tests

After the reaction, the solid catalyst was washed with 20 mL of methanol (2 mL/min) in the same reactor, and then calcined at 550 °C during 6 h in air. The catalytic experiments together with the analytics corresponding to the re-usability tests were performed in the same way as the common experiments already described at the beginning of Section 2.4.

3. Results and discussions

3.1. Catalysts characterization

A series of hydrotalcite-type (HTs) materials with different molar ratio M^{2+}/M^{3+}, copper loading close to 5 wt%, and surface areas of around 200 m^2/g were firstly synthesized and well characterized. Table 1 shows the main physicochemical and textural properties of Cu-based hydrotalcite-derived materials after calcination.

The structural characteristics of the Cu-based hydrotalcite-type materials were analyzed by XRD measurements. For the non-calcined Cu-HTs samples, the X-ray diffractograms of Fig. 1 show that a common Mg/Al layered hydrotalcite structure is obtained in practically all samples. Only in the case of 5.0%Cu-HT-1 sample, several diffraction peaks from aluminum hydroxide are observed. This is probably due to the large amount of Al^{3+} present in the initial solution, precipitated apart from the Cu-Mg-Al hydrotalcite and unable to enter inside the hydrotalcite structure during the co-precipitation process.

Table 1
Main physicochemical and textural properties of Cu-based HT-derived calcined materials with different M^{II}/M^{III} ratios.

Catalyst	Cu content (wt%)[a]	M^{II}/M^{III} molar ratio[a]	Surface area (m^2/g)[b] [BET method]
5.0%Cu-HT-1	4.9	1.0	218
5.0%Cu-HT-2	4.6	2.3	245
5.0%Cu-HT-3	4.9	3.3	212
5.0%Cu-HT-4	4.9	4.1	205
5.0%Cu-HT-5	5.1	5.5	224
5.0%Cu-HT-6	4.8	6.3	177

[a] Cu content and chemical composition measured by ICP.-
[b] Values calculated from N_2 adsorption isotherms by applying the BET method.

After the calcination of the Cu-based HT-precursors, the corresponding Cu-Mg-Al mixed oxides were attained, and their XRD patterns are drawn in Fig. 1b. For Cu-based mixed oxides the desired phase with poorly crystalline MgO structure containing the cationic species in the appropriate proportions has been obtained in practically all the measured materials, being necessary to emphasize the greater level of crystallization when increasing the Mg content. In the case of 5.0%Cu-HT-1 calcined sample, its X-ray diffractogram exhibits some peaks corresponding to aluminum oxide, as expected after analyzing the diffractogram belonging to the hydrotalcite precursor. It seems that after the calcination process some Al^{3+} from bayerite became part of the crystal lattice but other remained apart, giving rise to this aluminum oxide.

A second series of hydrotalcite-type materials having the same proportion (5.0 wt% with respect to the calcined material) of different transition metals, such as Cu, Co and Ni, and by fixing the molar ratio M^{2+}/M^{3+} equal to 4 were prepared and characterized. The main physicochemical and textural properties of 5.0%Cu-HT-4, 5.0%Co-HT-4, and 5.0%Ni-HT-4 calcined samples are summarized in Table 2. Chemical composition of this series of materials is again very similar to the theoretical one, while the attained surface areas are close to 200 m^2/g in the three cases.

As can be seen in Figure S1a (see SI), the XRD patterns of the three Cu-HT-4, Co-HT-4 and Ni-HT-4 as-prepared samples showed the characteristic peaks corresponding to the formation of well-crystallized layered double hydroxides of the hydrotalcite structure. Therefore, both the 5.0%Ni-HT-4 and the 5.0%Co-HT-4 samples contain the majority of either Ni^{2+} or Co^{3+} ions in the hydrotalcite structure partially substituting Mg^{2+} and Al^{3+} ions, respectively. In the case of Ni- and Co-based mixed oxides obtained after calcination of hydrotalcite precursors, the X-ray diffractograms of Figure S1b (see SI) only show the peaks corresponding to the formation of the MgO structure. This meaning that Ni^{2+} and Co^{3+} ions are well dispersed on the Mg-Al-O structure in both cases.

Finally, different hydrotalcite-type materials with a M^{II}/M^{III} molar ratio of ≈4 possessing different Cu loadings (from 1.0 to 12.8 wt%) were synthesized and characterized. The main physicochemical and textural properties of these Cu-based HT-4 calcined samples are detailed in Table 3, showing that the Cu was incorporated in the expected amounts into the hydrotalcite precursors, which maintain a M^{II}/M^{III} molar ratio around 4 and surface areas close to 200 m^2/g.

The XRD patterns of the Cu-based materials containing different Cu loadings before and after calcination treatment are depicted in Figure S2a and S2b (see SI), respectively. For these Cu-based series of samples, both the desired hydrotalcite phase and the mixed oxide phase with MgO structure are observed for the non-calcined and calcined material, respectively. Interestingly, even for the materials containing quantities of copper above 5.0 wt% non-isolated copper species are noticed.

In good agreement with what has been observed by XRD, microscopy analyses (SEM and HR-TEM) of the materials 5.0%Cu-HT-4, 10.0%Cu-HT-4 and 12.0%Cu-HT-4 (Fig. 2, and Figs. S6–8 in SI) confirm that the materials were, mostly, homogeneous, with a MgO structure, also showing a very high copper dispersion inside this crystalline structure. However, a very careful analysis by using HR-TEM allowed us to detect CuO_x nanoparticles in 12.0%Cu-HT-4 (Figure S16b). For materials containing lower copper loadings,

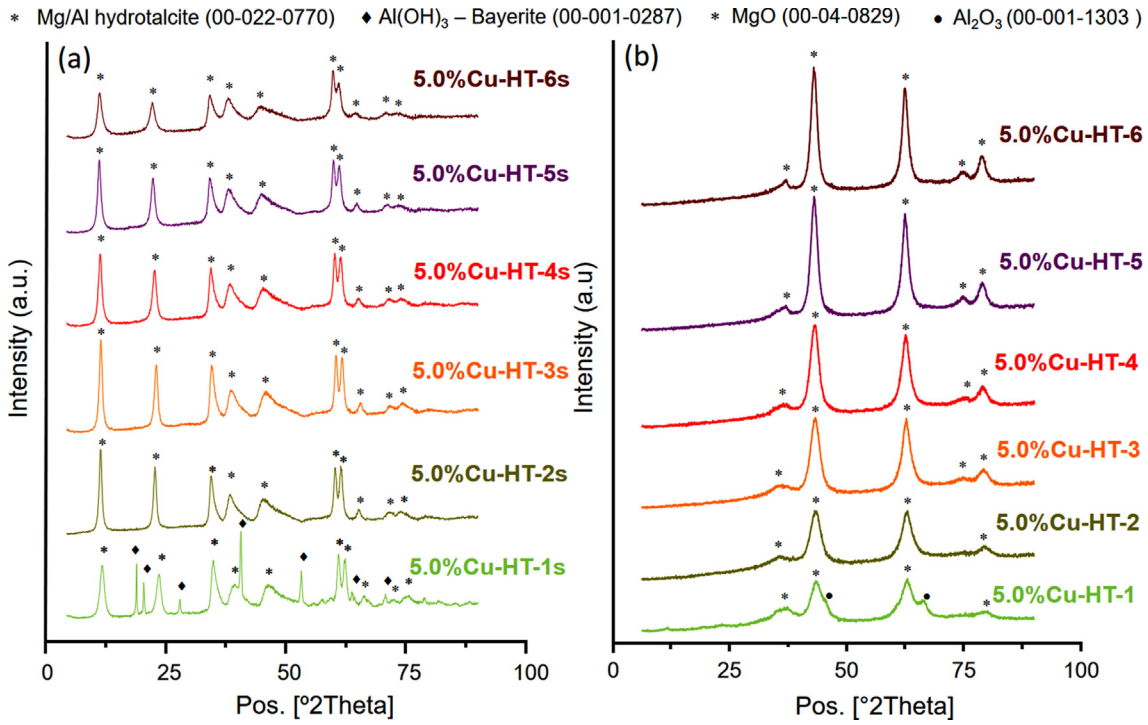

Fig. 1. (a) XRD patterns of as-synthesized Cu-based hydrotalcites with different M^{II}/M^{III} ratios (the "s" at the end of the name indicates a material analyzed just after the synthesis). (b) XRD patterns of Cu-based hydrotalcite-derived mixed oxides with different M^{II}/M^{III} ratios.

Table 2
Main physicochemical and textural properties of HT-derived calcined materials containing different transition metals.

Catalyst	Metal content (wt%)[a]	M^{II}/M^{III} molar ratio[a]	Surface area (m^2/g)[b] [BET method]
5.0%Cu-HT-4	4.9	4.1	205
5.0%Co-HT-4	4.9	4.2	198
5.0%Ni-HT-4	5.1	4.2	190

[a] Metal (Cu, Co or Ni) content and chemical composition measured by ICP.
[b] Values calculated from N_2 adsorption isotherms by applying the BET method.-

Table 3
Main physicochemical and textural properties of Cu-based HT-derived calcined materials with different copper loadings.

Catalyst	Cu content (wt%)[a]	M^{II}/M^{III} molar ratio[a]	Surface area (m^2/g)[b] [BET method]
HT-4	–	4.3	249
1.0%Cu-HT-4	1.0	4.4	196
2.5%Cu-HT-4	2.4	4.1	199
5.0%Cu-HT-4	4.9	4.1	205
7.0%Cu-HT-4	6.7	4.1	193
10.0%Cu-HT-4	9.9	4.2	196
12.0%Cu-HT-4	12.8	4.1	186

[a] Cu content and chemical composition measured by ICP.
[b] Values calculated from N_2 adsorption isotherms by applying the BET method.

those nanoparticles were not evident with this technique but, when using a more sensitive bulk technique such as NO adsorption (see Figure S9), again isolated CuO_x species became visible. Nonetheless, the XRD data together with the microscopic measurements evidence that most of the copper integrates the crystalline lattice in materials containing less than 12.0 wt% of Cu.

3.2. Catalytic results in continuous flow fixed-bed reactor

Catalytic experiments for selective dehydration of glycerol (GLY) to acetol were carried out as described in Experimental Section 2.4. In a first attempt aimed at optimizing the most important reaction conditions, different operational parameters, such as glycerol dilution and temperature, were varied by working always with 5.0%Cu-HT-4 calcined material as catalyst. The attained results in terms of catalytic activity (i.e. glycerol conversion), stability (maintenance of conversion with TOS), and more importantly, selectivity to acetol, were evaluated, main data being summarized in Table S1 (see SI) together with its more relevant discussion. From these results, the mixture MeOH/GLY = 90:10 (weight ratio) was selected as the optimal for further studies because it allows the system to work up to longer TOS with higher productivities of acetol, also maintaining a good catalyst stability. Once the optimum dilution degree of glycerol in methanol had been stablished, a series of experiments were done to figure out which temperature could improve both, glycerol conversion and selectivity to acetol. Tests of selective dehydration of glycerol over 5.0%Cu-HT-4 catalyst were carried out by varying temperature from 220 to 280 °C, keeping constant all the other reaction parameters (feed: MeOH/GLY = 90/10, flow = 2 mL/h, catalyst = 0.5 g, TOS = 9 h). The attained results are depicted in Figure S3 in terms of average conversion (cumulative conversion of glycerol during all the experiment, TOS = 1–9 h) and average selectivity to acetol (cumulative acetol selectivity during all reaction, TOS = 1–9 h). The temperature of 240 °C turned out to be the best by a small difference in terms of glycerol conversion and clearly better as far as selectivity to acetol is concerned during most part of the reaction. No great differences were noticed with respect to the catalyst stability.

Other important parameter to be considered is the particle size of the catalyst, which will determine whether we have our reaction being dominated by internal diffusion processes across the particle. We found that the internal diffusion controls the reaction when working with particle sizes above 0.600 mm, being the value

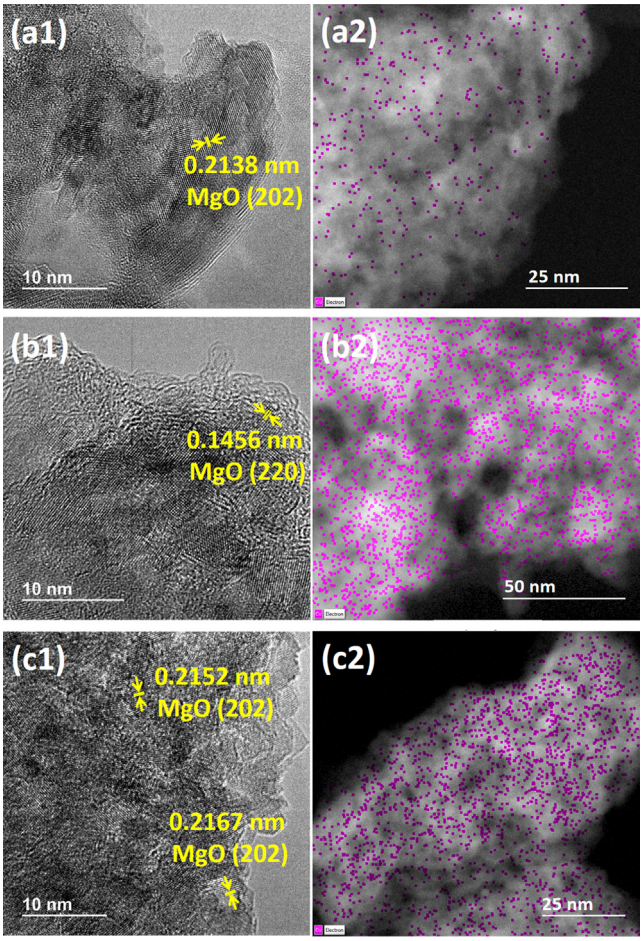

Fig. 2. HR-TEM (1) and STEM (2) images of (a) 5.0%Cu-HT-4, (b) 10.0%Cu-HT-4, (c) 12.0%Cu-HT-4. (■) Copper detected by EDS mapping.

0.425–0.600 the smallest one to be chosen to avoid load losses and reactor seals (see Figure S4 in SI). In addition, some experiments varying the liquid feed flow (q) along with the catalyst loading (W) were accomplished to prove that the liquid flow corresponding to 2 mL/h is in the area free of mass transfer limitations (see Figure S5 in SI). Thus, the set of experiments aimed to evaluate the catalytic performance of different hydrotalcite-derived mixed oxides can be carried out under these conditions (240 °C, MeOH/GLY = 90:10 wt, particle size = 0.425–0.600 mm, 2 mL/h). More information corresponding to these experiments can be found in the supporting information (SI).

The product distribution for the glycerol dehydration reaction under the aforementioned conditions and the reaction network proposed can be found in Fig. 3 and Scheme 2 (appearing in color all the identified compounds), respectively.

3.3. Optimizing the M^{II}/M^{III} molar ratio in Cu-based catalysts

As it has been already explained, thermal decomposition of Mg-Al hydrotalcite precursor yields a high surface area Mg-Al mixed oxide, which mainly exposes strong Lewis basic sites and some weak acid sites. The acid-base properties of these sites depend on the M^{II}/M^{III} molar ratio, i.e. mainly the Mg-Al ratio, in the hydrotalcite precursor [32–34]. With the aim of optimizing this M^{II}/M^{III} ratios in Cu-Mg-Al mixed oxides, hydrotalcites with (Cu + Mg)/Al ratios from 1 to 6 were prepared, calcined and tested in the selective dehydration of glycerol in continuous flow fixed-bed catalytic reactor. Catalytic results in terms of glycerol conversion and selectivity to acetol (at 240 °C and TOS = 4 h) attained for Cu-Mg-Al mixed oxides (5.0%-HTs) with different (Cu + Mg)/Al ratios are depicted in Fig. 4 and compared with CuO/Al_2O_3 and CuO/MgO (with 5 wt% Cu in both cases), as reference materials. In addition, the average both, glycerol conversion and acetol selectivity obtained for the different Cu-Mg-Al mixed oxides here studied during 9 h of reactor operation at 240 °C are also shown in Fig. 5. As can be seen, M^{II}/M^{III} molar ratios around 4 in the catalysts offered the highest both glycerol conversion and acetol selectivity (highest yield of acetol) achieved. The glycerol conversion and, more importantly, the acetol selectivity reached with 5.0%Cu-HTs catalysts with Mg/Al ratios from 3 to 5 are higher than the values achieved with CuO/Al_2O_3 reference material, while CuO/MgO material offered the worse results. However, the catalyst stability makes the difference between these values since Cu-Mg-Al materials with higher M^{II}/M^{III} molar ratios ((Cu + Mg)/Al ratios $\geq$4) are slightly more capable to keep the catalytic performance over at least 9 h.

Regarding the acid properties of the Cu-Mg-Al samples, looking at the NH_3-TPD profiles (Fig. 6a) two different peaks can be distinguished, the first one appearing at temperatures around 200 °C, and the second at temperatures above 350 °C. As it has been reported for calcined hydrotalcites, the acidity in-between this range can be ascribed to weak and moderate Lewis acid sites corresponding mainly to different Al^{3+} species [40,41], although a contribution of copper to the moderate acid sites cannot be discarded [42]. As far as the basic sites is concerned, the two peaks at lower temperatures appearing in Fig. 6b could be assigned to MgO (weak, physisorbed CO_2) and O^{2-} unsaturated (moderate, chemisorbed CO_2). Similar sites can be found in MgO [43].

Therefore, an explanation to the higher performance of these mixed oxides having M^{II}/M^{III} molar ratios between 3 and 4 could be found in the different distribution of active sites exhibited by each material, being more beneficial a material containing mainly weak Lewis acid sites and moderate Lewis basic sites. This adequate combination of Lewis acid and basic sites can be encountered in the aforementioned samples with M^{II}/M^{III} molar ratios ≈3-4 (see Fig. 6 and Table 4). On the contrary, higher ratios make the material lose both total acidity (concretely weak centers) and basicity, the former because of the lower aluminum loading, the latter due to the decrease of the vacancies in the mixed oxide structure produced by the presence of aluminum [34]. Nevertheless, the MgAl mixed oxides possessing a combination of Lewis both basic and acid sites but without Cu in the structure are not capable to perform the selective dehydration of glycerol to acetol. Thus, the presence of Cu is essential to carry out this process.

The presence of Cu in the hydrotalcite-derived mixed oxide provokes a decrease in the acidity and also in the basicity of the samples compared to the MgAl mixed oxides (see Table 4). This behavior can be explained by different effects occurring simultaneously. When Cu^{2+} replacing Mg^{2+} in the mixed oxide structure is close to Al^{3+} sites, Cu acts as the base but the acid site related to the Al is less acid with respect to the corresponding site in the only presence of Mg. Thus, the acidity (mainly week acidity) of the Cu-HT material is lower with respect to the acidity observed in the analogous HT sample without Cu (see also Table 5). In addition, by replacing Mg^{2+} by Cu^{2+} in the mixed oxide structure the amount and strength of basic sites are diminished in the material, mainly because CuO species have lower basicity than MgO species (see Table 5). Summarizing, the presence of Cu in MgAl mixed oxides lead to a decrease in the acidity and the basicity of the materials, being this effect more pronounced in the case of the basic properties. It is also possible that the Lewis acidity of the Cu^{2+} species could contribute to the total acidity presented by the Cu-HT samples, but this contribution should be quite minor in comparison to the amount of Al contained in the samples. In that case, the effect

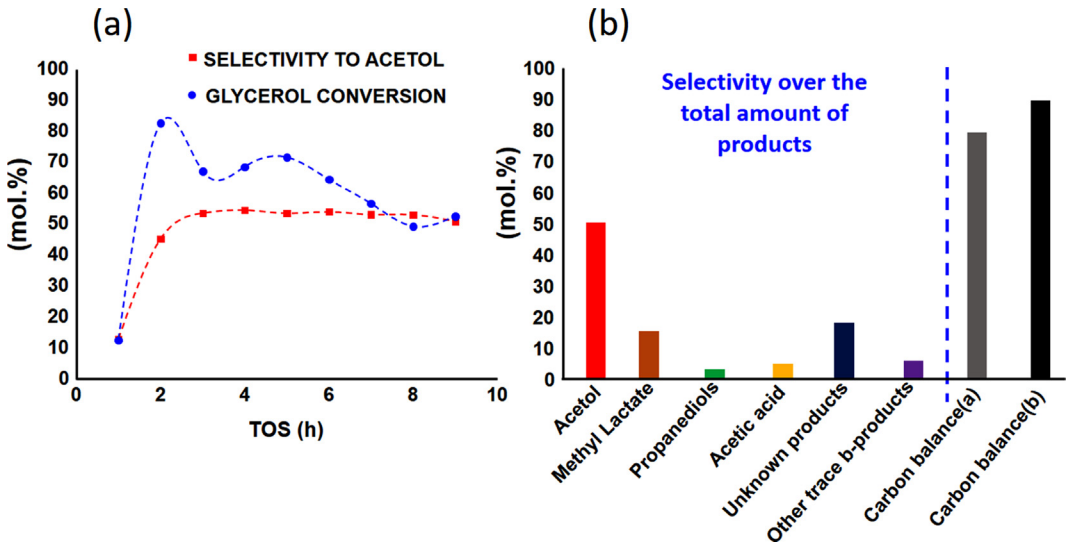

Fig. 3. (a) Glycerol conversion and selectivity to acetol with TOS under the optimal reaction conditions over the 5.0%Cu-HT-4 catalyst (b) Product distribution and carbon balance: [a]Carbon balance calculated with the total amount of products quantified during reaction, and [b]Carbon balance calculated including also the carbonaceous matter deposited on catalytic surface and the gas products coming from glycerol. (Reaction conditions: feed: MeOH/GLY = 90/10 wt, flow = 2 mL/h, temperature = 240 °C, catalyst = 0.5 g).

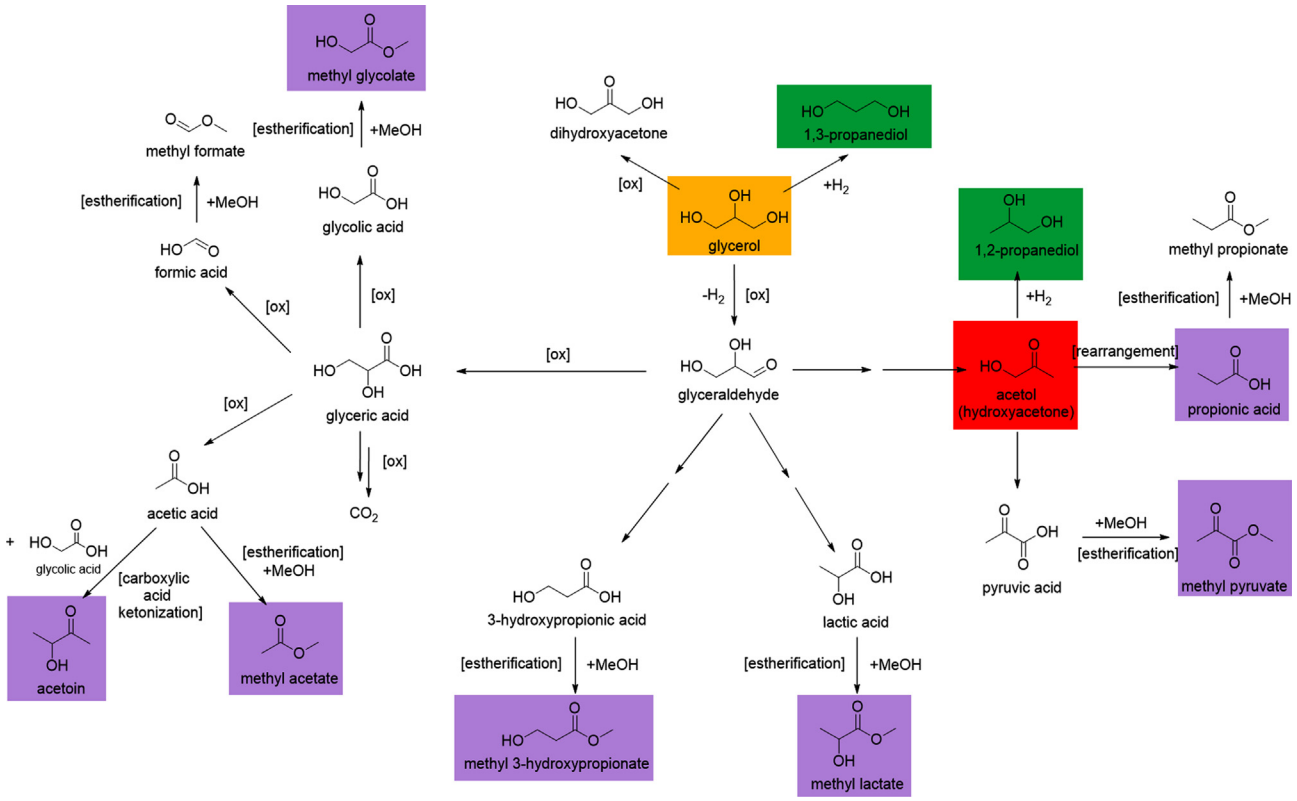

Scheme 2. Reaction network describing the different pathways when using 0.5 g of 5.0% Cu-HT-4 as catalyst under the following reaction conditions; T = 240C, Feed MeOH/Gly (9.1 wt), F = 2 mL/h, p.size = 0.425–0.600 mm. Colors correspond with detected products and match with colors of Fig. 3. (For interpretation of the references to colour in this figure legend, the reader is referred to the web version of this article.)

could be more relevant only in the case of Cu-HT samples with very low amount of Al (i.e. Cu-HT-6).

In summary, taking also into account the differences observed in Figs. 4–6, where the comparison between our Cu-based materials and CuO supported on Al_2O_3 and MgO, as well as with the pure MgAl mixed oxide (HT-4, Mg/Al = 4) is shown, a 5.0%Cu-HT-4 material having an adequate combination of weak acid and moderate basic sites presents a medium activity (in terms of glycerol conversion) between Al_2O_3-based (mainly acid) and MgO-based (basic) materials. With this 5.0%Cu-HT-4 material the best catalytic results (maximum values of selectivity and yield to acetol) can be reached. Therefore, weak acid sites corresponding to Al^{3+} can be concluded as the main responsible of the glycerol conversion as they are almost the only one present on the most active material

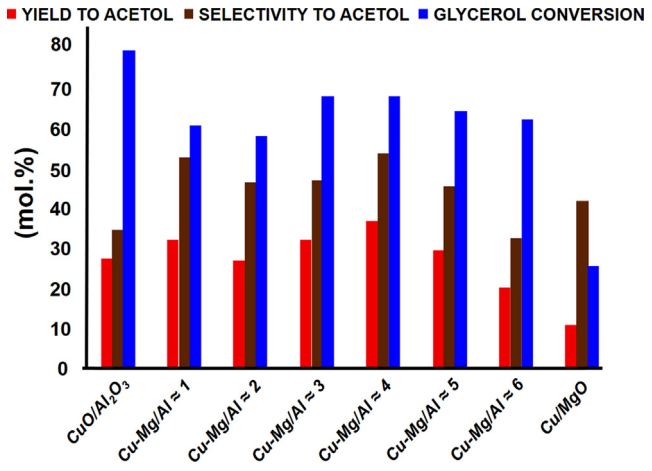

Fig. 4. Glycerol conversion, selectivity and yield to acetol in the selective dehydration of glycerol over 5.0%Cu-HT catalysts with different (Cu + Mg)/Al molar ratios at TOS = 4 h. (Reaction conditions: feed: MeOH/GLY = 90/10 wt, flow = 2 mL/h, temperature = 240 °C, catalyst = 0.5 g).

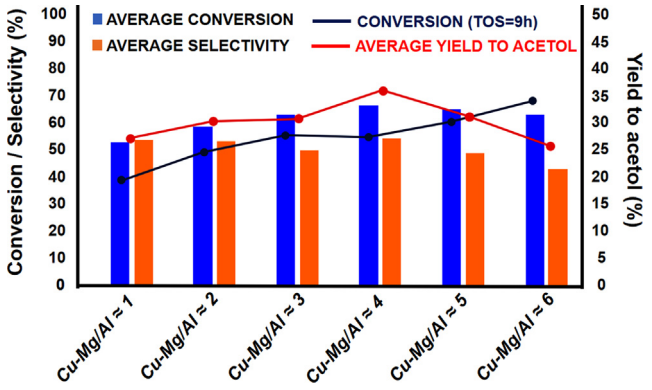

Fig. 5. Average glycerol conversion and selectivity to acetol in the selective dehydration of glycerol over 5.0%Cu-HT catalysts with different (Cu + Mg)/Al molar ratios during TOS = 1–9 h. (Reaction conditions: feed: MeOH/GLY = 90/10 wt, flow = 2 mL/h, temperature = 240 °C, catalyst = 0.5 g).

(CuO/Al_2O_3). This fact can be confirmed by the activity reached for MgO, without any acid site that was the worst among all the materials tested. In this sense, a compromise between acid and basic centers present in the solid seems to be needed for obtaining a good yield to acetol. On one hand, low Mg/Al molar ratios in the catalyst do not offer the necessary basicity to perform the reaction with good selectivity. On the other hand, higher Mg/Al ratios as well as pure MgO lack the acid site density needed to carry out the reaction with the desired acetol production.

Last but not least, and speaking about catalytic deactivation detected in these Cu-based catalysts, one possible explanation that fits in the tendency observed for these HT-derived materials would be the deactivation occurring on the weak acid sites, which ratio increases with decreasing of (Cu + Mg)/Al in the solids. However, with the handled data, the deactivation on the weak basic sites cannot be discarded either. Actually, it is impossible neither to distinguish between both options nor to discard any of them. Besides, there are literature reports making both acid and basic sites responsible for the catalytic deactivation in similar reactions, as coke formation would occur on acid sites, and polyglycerols or acetalization products of glycerol would be formed and remain adsorbed on basic sites [45].

Finally, as it was previously mentioned in this section, it is worth noting that the MgAl mixed oxide (HT-4), despite offering both weak acid and moderate basic centers, is not able to carry out the reaction in almost any extent (see Table 5), which unveils the need of having copper to interplay with glycerol through some interaction beyond a simple acid–base effect. This fact will be the subject of further discussions in next sections.

3.4. The role of Cu in Cu-Mg-Al mixed oxides

Apart from the results above-mentioned, when using other divalent transition metals with redox properties and a proven capability to produce acetol in the glycerol hydrogenolysis, such as nickel or cobalt [35,36,46,47], the results also revealed the need of using copper in this system (see SI, Table S3 and the explanatory text). This is in good agreement with what the majority of literature reports about glycerol transformation to propane-diols on the fact that copper is the essential metal when working with

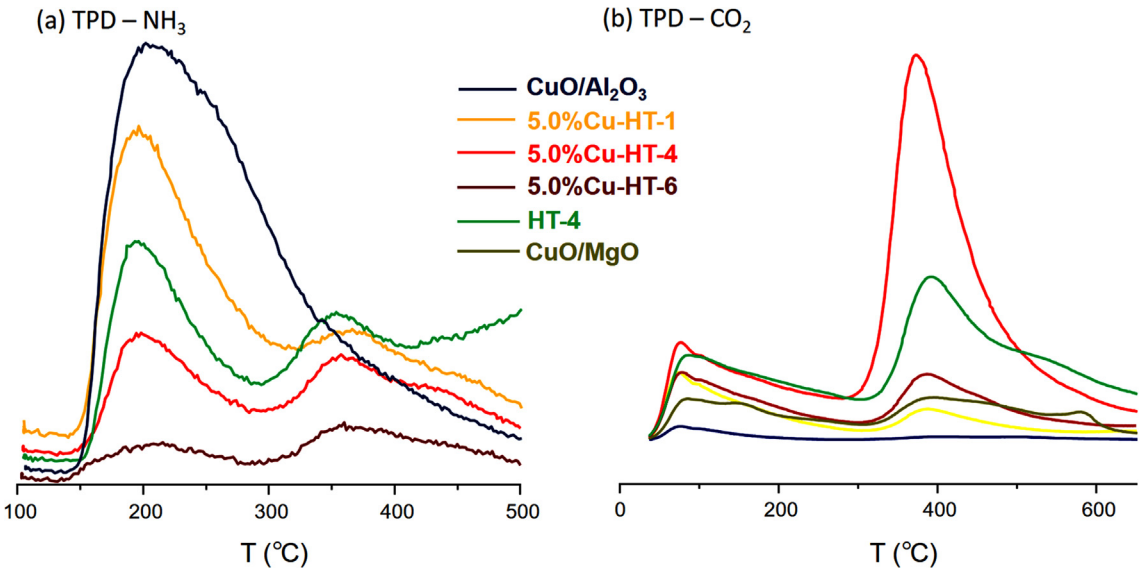

Fig. 6. NH_3 -TPD (a) and CO_2 -TPD (b) profiles of Cu-Mg-Al hydrotalcite-derived mixed oxides with different M^{II}/M^{III} ratios. Note: Baseline drift in HT-4 sample due to NO_x formation (T ≥ 450 °C).

Table 4
Quantitative data for temperature programmed desorption (NH_3-TPD and CO_2-TPD) of Cu-Mg-Al hydrotalcite-derived materials with different M^{II}/M^{III} molar ratios.

Catalyst	Acid site density (μmol/g)	Basic site density (μmol/g)	Acid sites (weak/medium)	Basic sites (weak/medium)
CuO/Al_2O_3	102	33	100	77:23
5.0%Cu-HT-1	122	111	68:32	66:34
5.0%Cu-HT-4	87	159	42:58	21:79
5.0%Cu-HT-6	63	153	37:63	44:56
CuO/MgO	–	111	-[a]	39:61

[a] MgO can be considered as having almost zero acidity [44].

Table 5
Comparison of NH_3 -TPD and CO_2 -TPD quantitative data and catalytic activity of hydrotalcite-derived Cu-Mg-Al and Mg-Al mixed oxides with the same Mg/Al ratio.

Catalyst	Acid sites (μmol/g) (weak:medium)	Basic sites (μmol/g) (weak:medium)	GLY conversion[a]	Selectivity to acetol[a]
5.0%Cu-HT-4	87 (42:58)	159 (21:79)	64.1	52.2
HT-4	124 (56:44)	245 (31:69)	6.9	39.0

[a] Average glycerol conversion and selectivity to acetol during TOS = 1–9 h. (Reaction conditions: feed: MeOH/GLY = 90/10 wt, flow = 2 mL/h, temperature = 240 °C, catalyst = 0.5 g).

metallic mixed oxides by using a fixed-bed reactor under close related reaction conditions [38,47]. Thus, the study of the different Cu species present in the Cu-based mixed oxide materials and how they specifically interact with the glycerol to selectively produce acetol becomes crucial to understand the catalytic process and the role of Cu in the solid material.

3.4.1. Effect of the oxidation state of Cu in Cu-Mg-Al mixed oxides

It has been reported that the coexistence of Cu^0, Cu^{1+} and Cu^{2+} species in a partially reduced Cu-Al oxide catalyst is responsible for its multifunctional role, thus catalyzing, for example, the simultaneous dehydration to acetol and the hydrogenolysis (hydrogenation) to 1,2-propanediol [38]. Therefore, the effects of having different copper species in our Cu-based mixed oxides were assessed by means of a detailed XPS study.

XPS experiments were performed by using: a) 5.0%Cu-HT-4, a fresh calcined material; b) 5.0%Cu-HT-4U, the same material recovered after reaction; c) 5.0%Cu-HT-4R, again the same material but this time reduced *"ex situ"* at 450 °C under H_2 atmosphere and without having been tested in reaction; and finally d) 5.0%Cu-HT-4R-INSITU, the same material but reduced at 450 °C under H_2 atmosphere in the instrument's own cell, to accurate that sample has not had contact with atmospheric air before being analysed. The attained results of XPS measurements are shown in Fig. 7 and summarized in Table 6. In addition, Figure S11 in the SI presents the XPS data attained by studying the stability (reduction) of the oxidation state of Cu on solid samples under measurement conditions. The results allow discarding the reduction of Cu species during these experiments.

In the fresh sample the $Cu2p_{3/2}$ main peak appears at 935.7 eV together with a shoulder at lower BE (932.6 eV). The presence of the shake-up satellite (s/m = 0.45) and the corresponding modified Auger Parameter of 1850.9 eV confirm the assignation as Cu^{2+} predominately [48], where the lower BE is related to a minor amount of reduced copper species (Cu^{1+}/Cu^0). The high BE shift of the Cu^{2+} ion (935.7 eV) is due to final state effects related to their high dispersion in the HT matrix [49]. An opposite situation is observed in the case of the used material (5.0%Cu-HT-4U), where the main peak appears at low BE (932.9 eV) together with a shoulder at high BE (935.6 eV). The lower shake-up intensity (s/m = 0.30) and the value of the modified Auger Parameter of 1849.5 eV indicate the presence of reduced copper species Cu^{1+} predominately, whereas the shoulder at high-BE corresponds to Cu^{2+}. On the other hand, in the case of the *"ex situ"* H_2 reduced sample (5.0%Cu-HT-4R) two peaks at 935.6 eV and 933.5 eV are observed, associated to Cu^{2+} and to reduced Cu^{1+}, respectively. The presence of reduced copper is confirmed by the value of the modified Auger Parameter at 1849.6 eV. Finally, in the *"in situ"* H_2 reduced sample (5.0%Cu-HT-4R-INSITU) two main peaks corresponding to Cu reduced species can be distinguished at 928.9 and 932.2 eV, and also one shoulder at 935.5 (Cu^{2+}). The value of the modified Auger Parameter at 1850.2 eV unveils the majority presence of Cu^0 versus Cu^{1+}. In addition, the splitting of the $Cu2p_{3/2}$ XPS peak into two components (928.9 and 932.2 eV) is related to differential charging of the sample because of the presence of Cu metal species in different environments and/or particle sizes. Small amounts of Cu^{2+} are also detected, based on the XPS component at BE of 935.5 eV and the shake-up peak.

The presence of Cu^{1+} in the 5.0%Cu-HT-4U used catalyst evidences that the reduction of Cu^{2+} species present in the fresh (calcined) sample is taking place during the reaction. However, since the used catalyst has been analysed after being exposed to atmospheric air and metallic copper (Cu^0) is easily oxidized into either Cu^{1+} or Cu^{2+} [50], the extent of copper species reduction through this *"on reaction"* reduction is difficult to define. The TPR analysis of the fresh (calcined) material and the *"ex situ"* H_2 reduced material (see Figure S12) also confirms the presence of Cu^{2+} species (peak at 285 °C) [51,52] in the former (5.0%Cu-HT-4) and segregated Cu^{2+} and/or Cu^{1+} species (peak at 190 °C) [53,54] in the later (5.0%Cu-HT-4R). Probably, both Cu^0 and Cu^{1+} are present in the reduced material 5.0%Cu-HT-4R. Cu^0 would be formed during the reduction with H_2 at 450 °C (see XPS Cu-HT4-R-INSITU, Fig. 7d), whereas Cu^{1+} would result from the oxidation of Cu^0 to Cu^{1+} in the presence of air (see XPS Cu-HT4-R, Fig. 7c). And, if the used material (5.0%Cu-HT4U) also suffers a reduction during the glycerol dehydration process, as it seems, this could also be applied to it.

With the aim of setting up if these reduced copper species detected in Cu-Mg-Al mixed oxides are active or not in the selective dehydration of glycerol, the 5.0%Cu-HT-4R (*"ex situ"* H_2 reduced) material having mainly Cu^{1+} species (see XPS data, Fig. 7 and Table 6) was tested in reaction, finding very similar activity (glycerol conversion) and selectivity to acetol values to those obtained with the original 5.0%Cu-HT-4 calcined or unreduced material (see Fig. 8). In addition, no significantly faster deactivation occurred at larger TOS for the reduced material compared to the calcined one. Another experiment with the 5.0%Cu-HT-4R-INSITU material (reduced in the same fix-bed catalytic reactor at 450 °C under H_2 atmosphere during 4 h, prior to the reaction), having mainly Cu^0 (see XPS data, Fig. 7 and Table 6), was

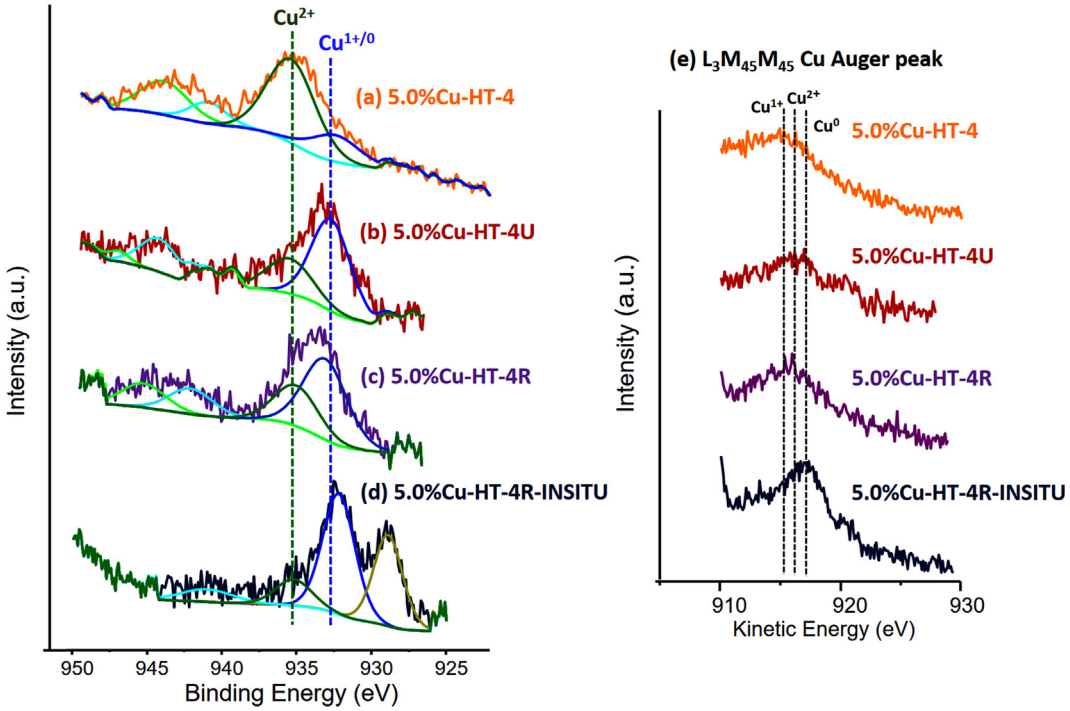

Fig. 7. $Cu2p_{3/2}$ XPS peak of (a) 5.0%Cu-HT-4 (fresh, calcined), (b) 5.0%Cu-HT-4U (used), (c) 5.0%Cu-HT-4R (H_2 reduced *"ex situ"*), (d) 5.0%Cu-HT-4R-INSITU (H_2 reduced *"in situ"*), (e) $L_3M_{45}M_{45}$ Cu Auger peak for the studied Cu-Mg-Al samples.

Table 6
XPS data of the $Cu2p_{3/2}$ core level and the surface composition.

Catalyst	Cu ($2p_{3/2}$)			α[a]	Molar ratio		Molar ratio
	B.E. (eV			(eV)	Cu^{2+}	$Cu^{1+/0}$	Cu: Al: Mg
	Cu^{2+}	$Cu^{1+/0}$	s/m				
5.0%Cu-HT-4	935.7	932.6	0.45	1850.9	84	16	2.4: 58.3: 39.3
5.0%Cu-HT-4U	935.6	932.9	0.30	1849.5	47	53	2.1: 56.2: 41.7
5.0%Cu-HT-4R	935.6	933.5	0.42	1849.6	47	53	1.6: 56.5: 41.8
5.0%Cu-HT-4R-INSITU	935.5	932.3/928.9	0.12	1850.2	20	80	1.2: 57.0: 41.7

[a] $Cu2p_{3/2}$ XPS (BE) + $L_3M_{45}M_{45}$ CuAES (KE).

carried out. In this case, a significant decrease in glycerol conversion was observed, falling the average value from ≈65% to ≈45% with respect to the other two samples discussed above. As for the acetol selectivity, also a lower value was obtained (from ≈50% to ≈45% in average) over this reduced sample mainly possessing Cu^0 species.

From the results obtained up to now, it is reasonable to think that the Cu^{2+} species originally present in the 5.0%Cu-HT-4 (calcined) catalyst at the beginning of the reaction are reduced "*in situ*" to Cu^{1+} and/or Cu^0 species throughout the glycerol dehydration process. The experiments herein described have set Cu^{1+} and Cu^{2+} appearing to be more active for this reaction than metallic copper, being the catalyst when the Cu is found mainly as Cu^0 much less active and slightly less selective towards acetol compared to the solids having majorly cationic Cu species.

3.4.2. Additional tests and measurements

In order to provide further insights into the role of copper species in the Cu-Mg-Al mixed oxides during the catalytic selective dehydration of glycerol in continuous flow fix-bed reactor, three additional experiments were carried out and the liquid and gaseous products were analyzed at the exit of the reactor. Gas composition was determined by using a specific GC-TCD system fitted with 3 detection lines for determination of H_2, N_2 and light hydrocarbons, while liquid composition was determined by the standard GC-FID system (see Experimental section).

For the first experience, the reactor previously charged with 5.0%Cu-HT-4 catalyst was fed for one hour only with absolute methanol (MeOH pre-treatment). The thus obtained results are shown in Fig. 9a. As can be seen, ≈30% of methanol fed is converted in the presence of Cu-Mg-Al material (mainly containing Cu^{2+} species) into gaseous products, such as CO, CO_2, and H_2, together with very low amounts of methyl-formate.

Then, the same 5.0%Cu-HT-4 catalyst (already pre-treated with MeOH at 200 °C) was fed with a mixture of GLY/Water (10/90 in weight) during 6 h, and the catalytic results were compared with another experiment performed by feeding a fresh 5.0%Cu-HT-4C catalyst (without the previous pre-treatment with methanol) with the same GLY/Water (10/90 wt) mixture during 6 h as well. The attained results are depicted in Fig. 9b, and they make clear the fact that the pre-treatment had beneficial effects on the catalytic performance. This could be attributed to the presence of either Cu(I) or Cu(0) instead of Cu(II) species, thanks to the hydrogen formation when feeding with MeOH during the catalyst's pre-treatment (see Fig. 9a). Thus, these copper reduced species would be more active than Cu^{2+} species for this reaction and, since Cu^{1+} has already been found to be more active than Cu^0 (Section 3.4.1, Fig. 8), Cu^{1+} can be concluded as the most active species for this reaction. These evi-

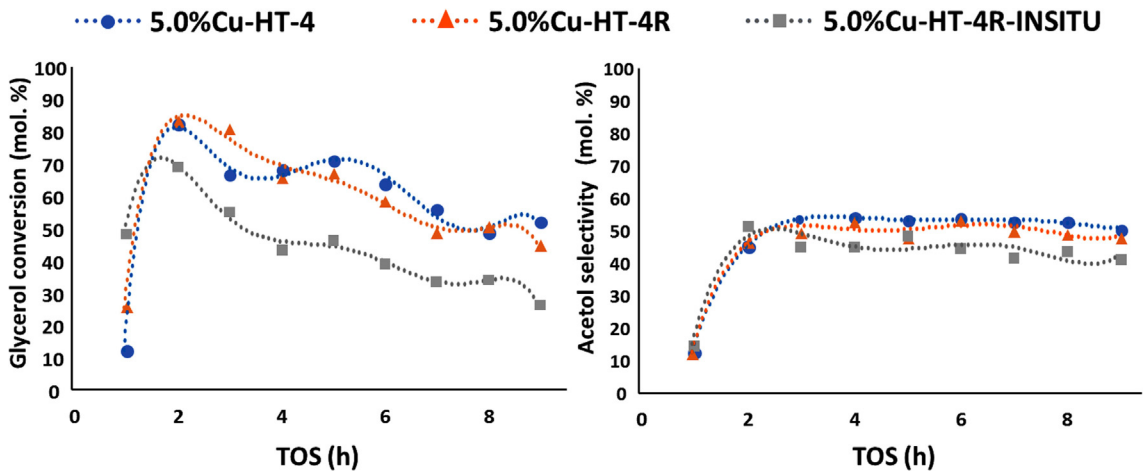

Fig. 8. Glycerol conversion (a) and selectivity to acetol (b) for 5.0%Cu-HT-4, 5.0%Cu-HT-4R and 5.0%Cu-HT-4R-INSITU materials. (Reaction conditions: Temperature = 240 °C, feed: MeOH/GLY (90/10 w.), flow = 2 mL/h, catalyst: 0.5 g).

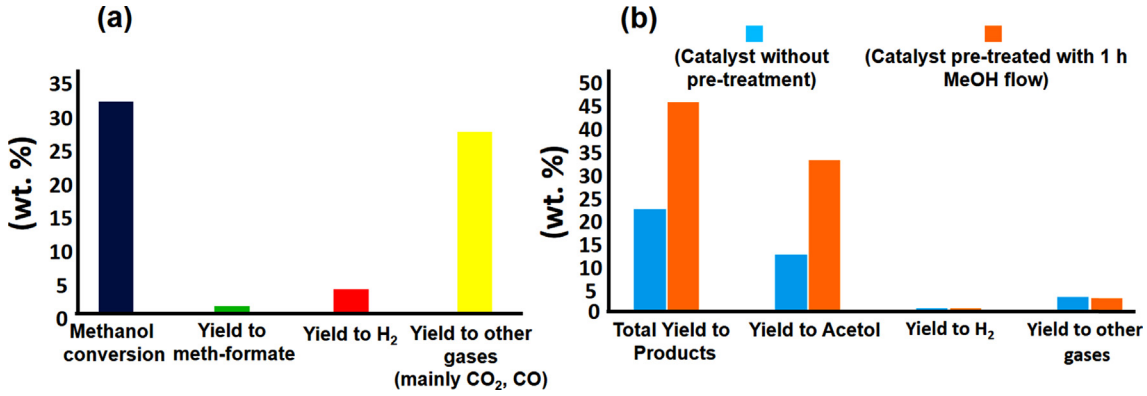

Fig. 9. (a) Pre-treatment test of 5.0%Cu-HT-4C catalyst with methanol (Reaction conditions: Feed: methanol, temperature = 240 °C, flow = 2 mL/h, catalyst: 0.5 g). (b) Catalytic results of selective glycerol dehydration over 5.0%Cu-HT-4 with and without methanol pre-treatment (Reaction conditions: Feed: water/glycerol (90/10 wt), temperature = 240 °C, flow = 2 mL/h, catalyst: 0.5 g).

dences are in good agreement with some recent results reported by Batiot-Dupeyrat and co-workers based on catalytic results together with DFT calculations [55].

TPR measurements of the 5.0%Cu-HT-4 calcined sample before and after pre-treatment with methanol (at 200 °C) unveils the oxidation of Cu(II) when comparing with the original calcined sample (Fig. 10). Therefore, it is reasonable to think that the methanol feeding used throughout this work is able to make the corresponding Cu(II) → Cu(I), Cu(0) transformation. In fact, during the pre-treatment with MeOH, approximately 25 mmol of H_2 were produced, as 0.4 mmol of copper are present in our catalyst, this quantity could be enough to reduce most of the Cu^{2+} species inside the catalyst.

In summary, under the reaction conditions here employed, the Cu^{2+} species present in the catalyst undergo the corresponding reduction to Cu^{1+} (and Cu^0) species, thanks to the presence of MeOH, favoring Cu^{1+} species the catalytic selective dehydration of glycerol to acetol. Although it is hard to distinguish between the presence of Cu^{1+} and Cu^0 due to the oxidation behavior of copper once exposed to the air, results shown in Fig. 8 point out Cu^{1+} as more active species to carry out the reaction than Cu^0.

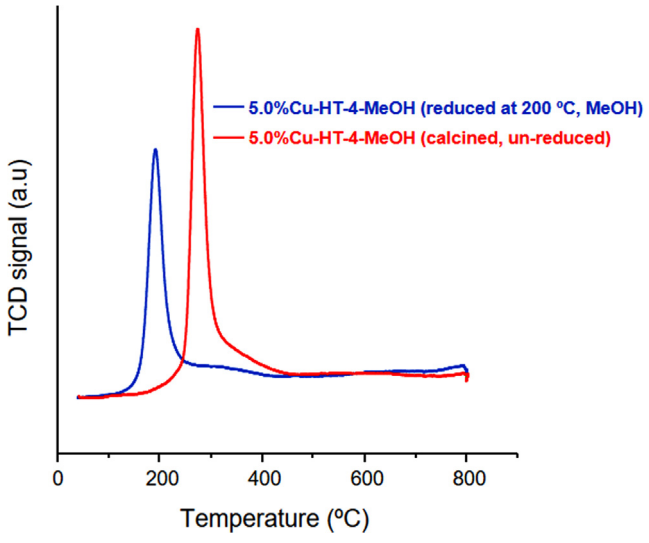

Fig. 10. TPR traces for 5.0%Cu-HT-4 (calcined, un-reduced) and 5.0%Cu-HT-4R (calcined + reduced at 200 °C with MeOH).

3.4.3. FT-IR measurements

In order to explain the catalytic behavior of the 5.0%Cu-HT-4 sample, and to provide further information about the reaction mechanism and the role of copper in the reaction pathways, IR spectroscopic studies have been performed using 1,2-propanodiol as probe molecule instead of glycerol. The selection of 1,2-propanediol (boiling point = 214 °C) as probe molecule respond only to an experimental reason, since the extremely high boiling

point of glycerol (290 °C) made impossible to properly work with it in gas phase in our FTIR system. In addition, the HT-4 (Mg/Al = 4), 5.0%Ni-HT-4 and 5.0%Co-HT-4 samples displaying much lower catalytic activity have also been analyzed. 1,2-propanodiol has been adsorbed at 25 °C on all samples until saturation coverage, and then the temperature has been stepwise increased from 25 °C to 160 °C, acquiring IR spectra at each temperature.

Gas phase 1,2 propanediol shows a complex set of IR bands in the low frequency region with maxima at 1654, 1137, 1079, 1043, 989, 924 and 839 cm^{-1}. After adsorption at 25 °C, the IR bands corresponding to the νC—O vibration (1137, 1079 and 1043 cm^{-1}) are shifted to higher frequencies (1143, 1085 and 1058 cm^{-1}) on all samples, in addition to a corresponding shift in the OH band of all samples (3730 cm^{-1}) to lower frequency (Fig. 11). Since the interaction of 1,2 propanediol is relatively strong in all cases (i.e. stable toward evacuation at 10^{-6} mbar and 25 °C) the red shift of the νC—O IR bands may correspond to an interaction with Lewis acid sites, besides that with OH groups. In addition, the shift in the νC—O IR bands is the same in all samples, indicating similar adsorption sites in all samples. This fits with what has been already pointed out about the weak acid sites corresponding to Al^{3+} as the main responsible of the catalytic activity. Since these acid sites are present in all the studied materials (see NH_3-TPD measurements, Figure S10 in SI), they could be the main responsible of the reactant adsorption.

Despite of this, by analyzing the evolution of the adsorbed 1,2-propanediol compound at increasing temperatures, a different behavior could be observed depending on the nature of the transition metal site (Cu, Ni, and Co), envisaging different reaction mechanisms and, accordingly, reaction intermediate species and reaction rates. Thus, in the 5.0%Cu-HT-4 sample increasing reaction temperature up to 160 °C leads to the appearance of a band at 1705 cm^{-1} corresponding to a carbonyl functional group, whereas under the same conditions in the Ni and Co based catalyst a band at 1596 cm^{-1} is observed corresponding to C=C bond, while no additional band could be observed in the HT-4 sample (Fig. 12). This may correspond to a different activation mode of the 1,2-propanediol, where a hydride abstraction could take place promoted by Cu species, whereas OH^- abstraction catalyzed by Lewis acid sites takes place on Ni and Co catalysts. Moreover, using CO as a probe molecule, Cu^{1+} species have been evidenced in the IR studies after 1,2-propanediol adsorption at 160 °C on the 5.0%Cu-HT-4 sample (IR band at 2098 cm^{-1})[56], which may be related to Cu^{2+} reduction by the aforementioned Cu-hydride interaction (Fig. 13). In opposite, no reduced species Ni^{1+} nor $Co^{2+/1+}$ have been observed in the 5.0%Ni-HT-4 and 5.0%Co-HT-4 samples under similar conditions. This fact was fully expected considering the very low reducibility of these samples, as very low amounts of Ni^{2+} and Co^{3+} are available to be reduced at low temperatures (see TPR, Figure S13 in SI). Thus, it can be concluded that weak acid centers are important because they are 1,2-propanediol adsorption centers (see NH_3-TPD, Figure S10 in SI), and that the additional presence of reducible centers, such as Cu^{2+} (but not Ni^{2+} and Co^{3+}), could favor the abstraction of H^-, thereby accelerating the carbonyl group formation pathway.

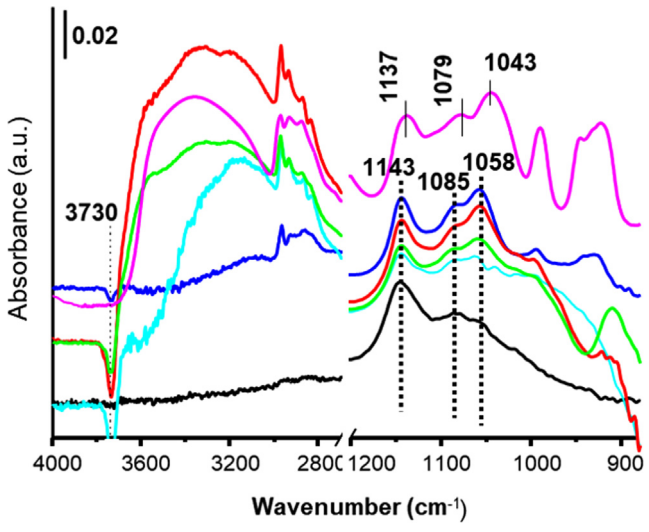

Fig. 11. IR spectra of 1,2-propanediol adsorbed at 25 °C on 5.0%Cu-HT-4 (blue), 5.0% Ni-HT-4 (red), 5.0%Co-HT-4 (green), HT-4 (cyan) and 5.0%Cu-HT-4R (ex situ H_2 reduced, black). In magenta gas phase IR spectra of 1,2-propanediol as reference spectra. (For interpretation of the references to colour in this figure legend, the reader is referred to the web version of this article.)

Once Cu^{2+} and Cu^{1+} are identified as the two main species present in the catalyst when the reaction is going on, and to assess if Cu^{2+} or Cu^{1+} are involved in the possible intermediate formation step, the 5.0%Cu-HT-4 sample has been *"ex situ"* reduced in H_2 flow (containing mainly Cu^{1+}, see XPS data of 5.0%Cu-HT-4R in Fig. 7) and analyzed in the IR study. As seen in the Cu-based non-reduced sample, a band at 1705 cm^{-1} due to the presence of carbonyl group has been observed in the 1,2-propanediol temperature dependent reaction profile. Nevertheless, the onset of carbonyl group formation appears at a slightly lower temperature, i.e. 120 °C, in the *"ex situ"* reduced sample versus 160 °C in the calcined sample (see Figure S14 in SI). Thus, while both Cu^{2+} and Cu^{1+} can be considered as active sites in the 5.0%Cu-HT-4 sample, a slightly higher reactivity could be observed for Cu^{1+}, which agrees on the improvement already seen when reducing the Cu-containing catalyst with MeOH at 240 °C (see Section 3.5.2). It is important to remark based on the IR data that the enhanced catalytic activity in the glycerol dehydration observed with 5.0%Cu-HT-4 sample can be ascribed to the specific role of copper versus other transition metals to promote the carbonyl group formation pathway at the beginning of the process.

However, despite displaying different reaction mechanisms, this cannot explain the markedly lower activity of 5.0%Co-HT-4 and 5.0%Ni-HT-4 catalysts. Another aspect which could influence the catalytic activity is the interaction strength of the reaction products with the catalyst surface, in a way that a stronger interaction would result in a fast catalyst deactivation. Thus, and in order to analyze the interaction strength of the reaction products, hydroxyacetone (or acetol) has been adsorbed on the 5.0%Cu-HT-4 and 5.0%Ni-HT-4 samples and followed by FT-IR spectroscopic measurements. As shown in Fig. 14, hydroxyacetone interacts on both catalysts, although the interaction is lower on the 5.0%Cu-HT-4 sample and stronger on the 5.0%Ni-HT-4 sample, probably because of the higher density of acid sites in this sample (see NH_3-TPD, Table S2 in SI).

Summarizing, it can be inferred that weak acid sites are relevant for adsorption of 1,2-propanediol, and the presence of specific copper sites in the Cu-HT sample could favor hydride abstraction in the first step of reaction. Moreover, Cu^{1+} species show a higher reactivity compared to Cu^{2+}, and since Cu^{2+} species are reduced in the first state of the reaction due to the presence of methanol, we can assess and confirm Cu^{1+} as active sites in the glycerol dehydration reaction over 5.0%Cu-HT-4 catalyst. Moreover, the desorption of reaction products is enhanced in the 5.0%Cu-HT-4 sample compared to the 5.0%Ni-HT-4 and 5.0%Co-HT-4 materials. This could be related to the different distribution of acid-base sites in both Co- and Ni-based samples (see NH_3-TPD measurements, Table S10 in SI) that could have too acid density, thus making problematic acetol to leave the catalytic surface. Thus, the essential role of copper species together with the higher interaction of the prod-

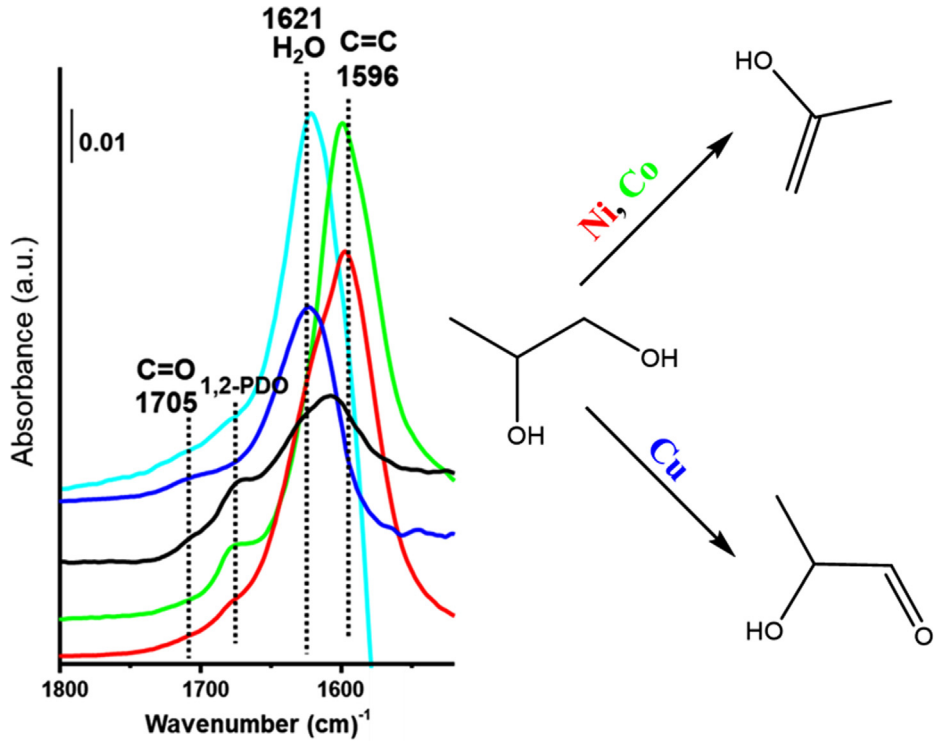

Fig. 12. IR spectra of 1,2-propanediol at 160 °C on 5.0%Cu-HT-4 (blue), 5.0%Ni-HT-4 (red), 5.0%Co-HT-4 (green), HT-4 (cyan) and 5.0%Cu-HT-4 *"ex situ"* H_2 reduced (black)1,2-PDO: IR peak related to 1,2-propanediol. (For interpretation of the references to colour in this figure legend, the reader is referred to the web version of this article.)

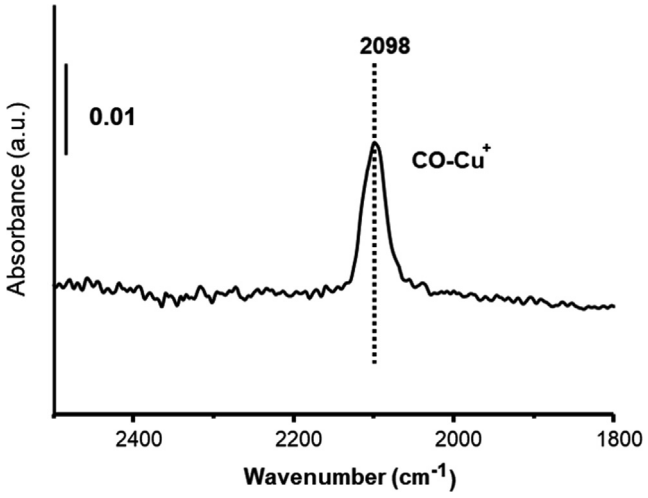

Fig. 13. IR spectra of CO adsorption at 25 °C as probe molecule on the 5.0%Cu-HT-4 sample after 1,2-propanediol adsorption and increasing temperature to 160 °C.

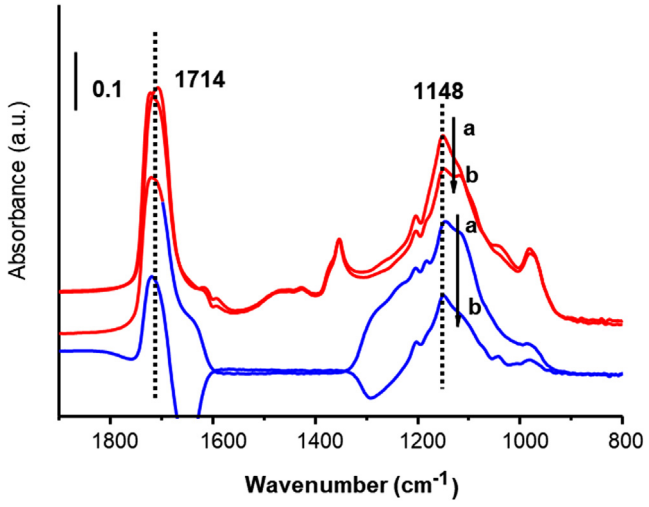

Fig. 14. IR spectra of hydroxyacetone adsorbed at 25 °C on 5.0%Cu-HT-4 (blue) and 5.0%Ni-HT-4 (red) (a), and after evacuation at 25 °C for 5 min (b). (For interpretation of the references to colour in this figure legend, the reader is referred to the web version of this article.)

ucts on the Co- and Ni-based catalysts may explain the markedly higher catalytic activity observed with the Cu-containing catalyst.

3.4.4. Proposed mechanism

The foregoing results indicated that Cu is essential to achieve good conversion and selectivity to acetol, mainly due to the formation of an intermediate possessing a carbonyl group at the beginning of the process. In this sense, glyceraldehyde should be the intermediate reaction, following the results getting by the FT-IR study. In Scheme 3 a possible reaction pathway is shown. In order to clarify, even more, the role of Cu and to elucidate some insights of the mechanism, catalytic activity tests of acetol formation with a low percent of glyceraldehyde into the starting feed were carried out.

This reaction was performed over the most active material that was 5.0%Cu-HT-4 so far, under similar conditions used before. They were followed by ^{13}C NMR at short reaction time, 45 min, observing the presence of a low amount of glyceraldehyde (see Figure S21 in SI). Because of the glyceraldehyde nature that gives a very high reactivity in that reaction medium, it was impossible to isolate or accumulate more quantity of glyceraldehyde during reaction; therefore, ^{1}H NMR data were unclear.

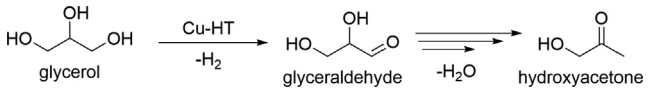

Scheme 3. Proposed reaction pathway for acetol formation over Cu-HT catalyst.

Experiments in continuous flow carried out with the less active catalyst Co-HT showed an improvement in the yield towards acetol when the fixed bed reactor was fed with the mixture of glycerol + 0.45 wt% glyceraldehyde (Fig. 15). This improvement has the same percentage value as the amount introduced on the feed: 0.45%. In these cases, it was necessary to use a small amount of water to dissolve the glyceraldehyde in the initial mixture.

These results gave us a useful proof about the mechanism of the reaction: Co is unable to activate the C-OH bond of glycerol towards the formation of glyceraldehyde, the intermediate to acetol. However, skipping the first step, Co-HT was able to transform glyceraldehyde to acetol.

3.5. Effect of the amount of Cu in Cu-based catalysts

Once the adequate Cu-Mg-Al mixed oxide with the optimal Mg/Al molar ratio was stablished as the best catalyst for the selective dehydration of glycerol to acetol, the effect of the amount of Cu in these materials was studied. Cu loading was varied from 0.0 to 12.0 wt%, finding out that, although the selectivity to acetol is barely affected when increasing the quantity of copper, the more copper the solid contains, the higher both conversion and yield to acetol are attained. Nonetheless, this is only true until reaching Cu loading of 10 wt% (see Fig. 16, and Table S4 in SI). From this amount of copper onwards, no further increase is observed for the glycerol conversion and the selectivity to acetol. Thus, a mixed oxide containing 10.0 wt% of copper would correspond to the optimal composition. The 10.0%Cu-HT-4 catalyst kept a good compromise between glycerol conversion and acetol selectivity and, more importantly, it provided the best catalytic stability during 9 h of reaction with practically no variation in the selectivity to acetol (≈55%, see Figure S15 in SI).

Comparison of the acidity and basicity data obtained by means of TPD analysis of both 5.0%Cu-HT-4 and 10.0%Cu-HT-4 calcined samples (see Table S5, in SI) show that the introduction of more copper into the structure does not affect significantly the amount and force of the active acid-basic centers. In fact, the two Cu-based materials exhibit almost the same acid/basic sites distribution, being slightly more acid and less basic the one containing lower amounts of copper (5.0%Cu-HT-4 sample). Therefore, we can associate higher activity observed for 10.0%Cu-HT-4 catalyst with increasing quantities of copper, as no effect of this greater amount of copper in the acid-basic properties of our materials was observed. In this sense, it was noticed that the more copper the material has, the more reducible it is and, therefore, a higher amount of copper is available to carry out the reaction. Nevertheless, once the 10 wt% of Cu is surpassed, part of the copper needs higher temperatures to be reduced (see Figure S16a, SI), thereby showing more difficulties to take part in the reaction. The position of this TPR peak, together with the CuO_x nanoparticles seen for the material 12.0%Cu-HT-4 in the HR-TEM measurements (Figure S16b, SI) made us thing about large aggregates of CuO_x as the responsible of this behavior [54].

3.6. Importance of the use of MeOH as solvent

Results up to now attained make necessary to remark that the choice and use of methanol as solvent for the selective dehydration of glycerol is a key parameter. Methanol is helping to reduce Cu^{2+} to Cu^{1+}, which has already been pointed out as the most active species in this process (see Sections 3.4.1 and 3.4.2). Thus, the presence of methanol facilitates the reaction occurrence. In this sense, several reactions for the selective dehydration of glycerol to acetol were performed to study the effects of the inclusion of water in the feed. Water was added to the GLY/MeOH mixture to evaluate if it could eventually replace, at least partially, the use of MeOH as solvent. Figure S18 summarizes the glycerol conversion results for different water additions to the system. The presence of added water resulted in a decrease in the amount of glycerol converted. It was also observed that the introduction of water had a significant effect on the catalyst stability. In conclusion, when the activity of the catalyst reaches a maximum in almost all cases, the overall yield of the reaction significantly decreases as soon as there is even a small quantity of water in the reaction medium.

This phenomenon could be explained not only because of the total or partial absence of methanol, but also taking into account the rehydration of the hydrotalcite-type material when water is introduced into the reaction media, water molecules could block acid centers needed for the first glycerol adsorption [57]. Neverthe-

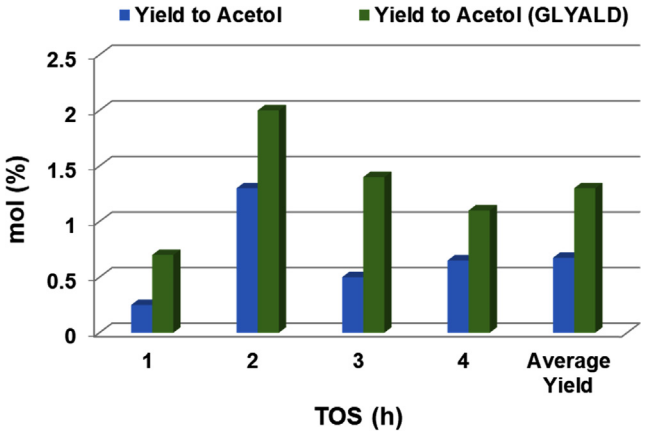

Fig. 15. Catalytic results of selective glycerol dehydration over 5.0%Co-HT-4 with (orange) and without (blue) glyceraldehyde co-feed (Reaction conditions: Feed: methanol/glycerol/glyceraldehyde/water (87.8/9.5/0.45/2.2 wt), temperature = 240 °C, flow = 2 mL/h, catalyst: 0.5 g). (For interpretation of the references to colour in this figure legend, the reader is referred to the web version of this article.)

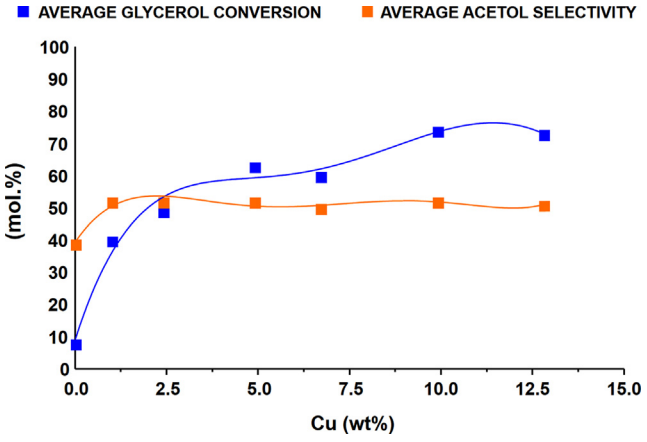

Fig. 16. Average glycerol conversion and average acetol selectivity for Cu-Mg-Al calcined materials with different Cu contents during TOS = 1–9 h (Reaction conditions: feed = methanol/glycerol (90/10 in weight), flow = 2 mL/h, with 0.5 g of catalyst at 240 °C).

less, the formation of the corresponding Cu-Mg-Al hydrotalcite phase was not detected, even for the reaction carried out in pure water (see Figure S19 in SI). Then, other possibility could be the effect that water could exert on the thermodynamic equilibrium.

3.7. Re-usability

The 10.0%Cu-HT-4 catalyst showed high catalytic activity accompanied with good selectivity to acetol in the selective dehydration of glycerol in continuous flow fixed bed reactor, although some deactivation was observed with time on stream. At this point, the question is if the Cu-Mg-Al material could be used several times in the reaction, for example by introducing regeneration cycles in-between reactions. To address this issue, catalyst recycles were carried out by washing the catalyst used in the reaction with MeOH, and then regenerating it under the same calcination conditions used for the fresh material (before its 1st use). Five consecutive re-uses of the 10%Cu-HT-4C catalyst with the preceding catalyst regenerations in each case were performed under standard reactions conditions for the selective glycerol dehydration and the attained results are given in Fig. 17. In general, both glycerol conversion and selectivity to acetol values remain practically unaltered during the five consecutive catalytic re-uses.

The issue of possible leaching of metallic species (i.e. Cu, Mg and Al) together with the deposition of carbonaceous compounds during the catalyst re-cycling tests was assessed by means of different comparative analysis of the catalysts before and after re-uses. Thus, thermogravimetry (TGA) and elemental (EA) analysis, together with ICP and surface area measurements of 5.0%Cu-HT-4 and 10.0%Cu-HT-4 re-used materials reveal that our Cu-Mg-Al materials are mainly deactivated by carbonaceous matter deposition, this making possible the recovering of the initial catalytic performance by means of a calcination process (see Tables S6 and S7 in SI). Any significant metal leaching was detected for both 5.0%Cu-HT-4 and 10.0%Cu-HT-4 catalysts after several re-uses, while after a primary surface area loss during the first use the surface area values stabilize around 150 m^2/g (Table S7 in SI). Besides that, it is necessary to point out that the reduction $Cu^{2+} \rightarrow Cu^{1+}/Cu^0$ already observed during the reaction does not affect the catalytic performance as Cu^{1+} are the most active species, as it has been already discussed in previous sections. Furthermore, the rehydration of the calcined hydrotalcite, due to the extensively described "memory effect" [57], could also have a role in the catalytic deactivation. However, a retrotopotactic transformation when feeding the reactor with a mixture containing small amount of water (see Figure S19) was not noticed, even though when water is generated throughout the reaction. The only structural difference observed after the reaction is the formation of a very small amount of CuO, probably growing from the mixed oxide phase and sintering during the reaction (see Figure S20). Nevertheless, this effect does not affect the re-uses of the material. All these observations let us to conclude that the carbonaceous compounds deposition on the solid surface could be considered, at this stage, as the main cause of catalyst deactivation in this process.

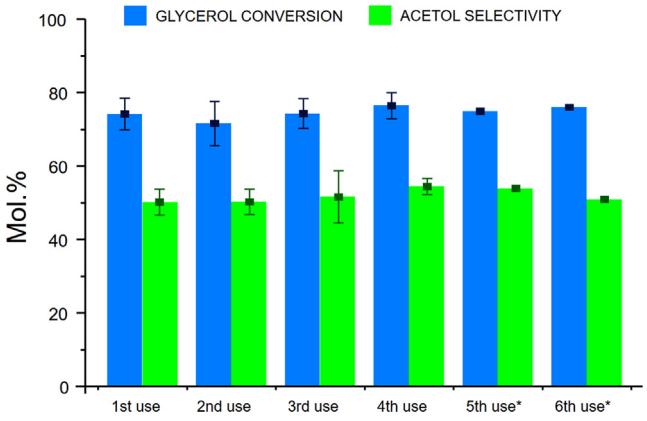

Fig. 17. Glycerol conversion and acetol selectivity accumulative data during reusability tests of 10.0%Cu-HT-4 catalyst (Average values of four repetitions). Reaction conditions: feed = MeOH/GLY (90/10 in weight), flow = 2 mL/h, with 0.5 g of catalyst at 240 °C. * For uses 5th and 6th only one experiment was carried out, therefore no error bars are presented.

Summarizing, Cu-Mg-Al materials have demonstrated to be highly active, selective, and also re-usable in the selective dehydration of glycerol in a continuous flow fixed bed reactor. Besides that, the catalysts remained active after several re-uses by introducing regeneration cycles in-between reactions and preserved their chemical and structural properties at least after five consecutive re-uses.

4. Conclusions

This research indicates that waste by-product glycerol from biodiesel production can be transformed into acetol by using environmentally friendly Cu-based mixed oxides derived from hydrotalcites as catalysts. Additionally, the reaction is carried out in a continuous flow fix-bed reactor, which could be scaled up from an industrial point of view. Concretely, the 10.0%Cu-HT-4 catalyst offered the best results for glycerol conversion (≈80%) and acetol selectivity (≈60%), being stable for 9 h. This type of catalysts showed similar results (yield ≈40%) when comparing with other materials with similar copper loadings, such as the recently described Cu-MgF_2. However, more importantly, the here optimized catalyst successfully addressed the relevant reusability issue. Thus, the catalyst remains active after several re-uses by introducing regeneration cycles in-between reactions and preserving their chemical and structural properties at least after two consecutive re-uses. Together with the development of a new alternative system to produce acetol from glycerol, interesting contributions to understand the reaction mechanism have been done. The experiments carried out to evaluate the effect on the catalytic performance of copper have pointed out this metal is essential to perform the glycerol dehydration to acetol with a high reaction rate. Probably, the preferred formation of a C=O containing intermediate makes the difference between Cu and Co or Ni. In this sense, Cu^{1+} has been concluded as the most active Cu species present in the catalyst, these species being formed at the beginning of the reaction by reduction of Cu^{2+} species. However, minor contributions to the reaction of the other two Cu-species (Cu^0 and Cu^{2+}) cannot be discarded. As far as the acid-base sites role is concerned, glycerol adsorption takes place on weak acid centers and then, once copper has interacted with the molecule and the intermediate is formed, and acid-base pair interaction would be responsible for the final generation of acetol.

Declaration of Competing Interest

The authors declare that they have no known competing financial interests or personal relationships that could have appeared to influence the work reported in this paper.

Acknowledgments

Financial support by Spanish Government (CTQ-2015-67592, PGC2018-097277-B-100 and SEV-2016-0683) and PhosAgro/UNESCO/IUPAC Partnership (Proj. 139) is gratefully acknowledged.

J.M. also thanks Spanish Government (CTQ-2015-67592) for his FPI fellowship.

Appendix A. Supplementary material

Supplementary data to this article can be found online at https://doi.org/10.1016/j.jcat.2020.03.010.

References

[1] BP Statistical Review of World Energy, #BPstats. 40 (2015). bp.com/statisticalreview.
[2] M. Stöcker, Angew. Chem. Int. Ed. 47 (48) (2008) 9200–9211.
[3] G.W. Huber, S. Iborra, A. Corma, Chem Rev. 106 (2006) 4044–4098.
[4] G.W. Huber, A. Corma, Angew. Chem. Int. Ed. 46 (2007) 7184–7201.
[5] J.N. Chheda, G.W. Huber, J.A. Dumesic, Angew. Chem. Int. Ed. 46 (2007) 7164–7183.
[6] A. Demirbas, Energy Convers. Manage. 50 (2009) 2239–2249.
[7] A.L. Moreira, J.M. Dias, M.F. Almeida, M.C. Alvim-Ferraz, Energy Fuels 24 (2010) 5717–5721.
[8] J. Costa, M. Almeida, M. Alvim-Ferraz, J. Dias, Energy Convers Manage. 74 (2013) 17–23.
[9] J.M. Dias, M.C. Alvim-Ferraz, M.F. Almeida, Bioresour. Technol. 100 (2009) 6355–6361.
[10] S.C. D'Angelo, A. Dall'Ara, C. Mondelli, J. Pérez-Ramírez, S. Papadokonstantakis, ACS Sust. Chem. Eng. 6 (2018) 16563–16572.
[11] G.M. Lari, G. Pastore, M. Haus, Y. Ding, S. Papadokonstantakis, C. Mondelli, J. Pérez-Ramírez, Energy Environ. Sci. 11 (2018) 1012–1029.
[12] D.T. Johnson, K.A. Taconi, Environ. Prog. 26 (2007) 338–348.
[13] C.C. Zhou, J.N. Beltramini, Y. Fan, G.M. Lu, Chem. Soc. Rev. 37 (2008) 527–549.
[14] T. Werpy, G. Petersen, A. Aden, J. Bozell, J. Holladay, J. White, A. Manheim, Top value-added chemicals from biomass, Volume 1-Results of screening for potential candidates from sugars and synthesis gas, Report of U.S. DOE, Energy Efficiency and Renewable Energy, Biomass, 2004.
[15] M.J. Climent, A. Corma, P. De Frutos, S. Iborra, M. Noy, A. Velty, P. Concepción, J. Catal. 269 (2010) 140–149.
[16] C. Vieville, J. Yoo, S. Pelet, Z. Mouloungui, Catal. Lett. 56 (1998) 245–247.
[17] R.R. Soares, D.A. Simonetti, J.A. Dumesic, Angew. Chem. 118 (2006) 4086–4089.
[18] N. Rahmat, A.Z. Abdullah, A.R. Mohamed, Renew. Sust. Energy Rev. 14 (2010) 987–1000.
[19] B. List, J. Am. Chem. Soc. 122 (2000) 9336–9337.
[20] W. Notz, B. List, J. Am. Chem. Soc. 122 (2000) 7386–7387.
[21] M.A. Dasari, P. Kiatsimkul, W.R. Sutterlin, G.J. Suppes, Appl. Catal. A:Gen. 281 (2005) 225–231.
[22] C. Chiu, M.A. Dasari, G.J. Suppes, W.R. Sutterlin, AIChE J. 52 (2006) 3543–3548.
[23] T.P. Braga, N. Essayem, S. Prakash, A. Valentini, J. Braz. Chem. Soc. 27 (2016) 2361–2371.
[24] S. Sato, M. Akiyama, R. Takahashi, T. Hara, K. Inui, M. Yokota, Appl. Catal. A: Gen. 347 (2008) 186–191.
[25] M. Velasquez, A. Santamaria, C. Batiot-Dupeyrat, Appl. Catal. B:Environ. 160 (2014) 606–613.
[26] A. Talebian-Kiakalaieh, N.A.S. Amin, H. Hezaveh, Renew. Sust. Energy Rev. 40 (2014) 28–59.
[27] M. Pagliaro, M. Rossi, Chem. Sus. Chem. 1 (2008), 653-653.
[28] A.K. Kinage, P.P. Upare, P. Kasinathan, Y.K. Hwang, J. Chang, Catal. Comm. 11 (2010) 620–623.
[29] D.C. Carvalho, L.G. Pinheiro, A. Campos, E.R.C. Millet, F.F. de Sousa, J.M. Filho, G. D. Saraiva, E.C. da Silva Filho, M.G. Fonseca, A.C. Oliveira, Appl. Catal. 471 (A: Gen. 2014,) 39–49.
[30] W.T. Reichle, Solid State Ion. 22 (1986) 135–141.
[31] D. Tichit, B. Coq, Cattech. 7 (2003) 206–217.
[32] F. Cavani, F. Trifirò, A. Vaccari, Catal. Today. 11 (1991) 173–301.
[33] J. Di Cosimo, V. Díez, M. Xu, E. Iglesia, C. Apesteguía, J. Catal. 178 (1998) 499–510.
[34] B.F. Sels, D.E. De Vos, P.A. Jacobs, Cat. Rev. 43 (2001) 443–488.
[35] R.L. Manfro, T.P. Pires, N.F. Ribeiro, M.M. Souza, Catal. Sci. Technol. 3 (2013) 1278–1287.
[36] M. Araque, L.M. Martínez, J.C. Vargas, M.A. Centeno, A.C. Roger, Appl. Catal. B: Environ. 125 (2012) 556–566.
[37] A. Bienholz, H. Hofmann, P. Claus, Appl. Catal. A:Gen. 391 (2011) 153–157.
[38] R.B. Mane, C.V. Rode, Green. Chem. 14 (10) (2012) 2780–2789.
[39] N. Blanch-Raga, A.E. Palomares, J. Martínez-Triguero, G. Fetter, P. Bosch, Ind. Eng. Chem. Res. 52 (2013) 15772–15779.
[40] J.Y. Shen, M. Tu, C. Hu, J. Solid State Chem. 137 (1998) 295–301.
[41] D. Yuan, X. Li, Q. Zhao, J. Zhao, S. Liu, M. Tadé, Appl. Catal. A:Gen. 451 (2013) 176–183.
[42] M. Trombetta, G. Ramis, G. Busca, B. Montanari, A. Vaccari, Langmuir 13 (1997) 4628–4637.
[43] M.D. Romero, J.A. Calles, M.A. Ocaña, J.M. Gómez, Microp. Mesop. Mater. 111 (2008) 243–253.
[44] I. Popescu, N. Tanchoux, D. Tichit, I.C. Marcu, Appl. Catal. A: Gen. 538 (2017) 81–90.
[45] P. Lauriol-Garbay, J. Millet, S. Loridant, V. Bellière-Baca, P. Rey, J. Catal. 280 (2011) 68–76.
[46] S. Mészáros, J. Halász, Z. Kónya, P. Sipos, I. Pálinkó, Appl. Clay Sci. 80 (2013) 245–248.
[47] X. Guo, Y. Li, W. Song, W. Shen, Catal. Lett. 141 (2011) 1458–1463.
[48] V.A. Naumkin, A. Kraut-Vass, S.W. Gaarenstroom, C.J. Powell, NIST standard reference database 20, version 4.1. https://srdata.nist.gov/xps/WagnerPlot.aspx.
[49] W. Grünert, N.W. Hayes, R.W. Joyner, E.S. Shpiro, M.R.H. Siddiqui, G.N. Baeva, J. Phys. Chem. 98 (1994) 10832–10846.
[50] P. Keil, D. Lützenkirchen-Hecht, R. Frahm, AIP Conf. Proc. 882 (2007) 490–492.
[51] L. Chmielarz, P. Kuśtrowski, A. Rafalska-Łasocha, R. Dziembaj, Thermochim. Acta 395 (2002) 225–236.
[52] S. Kannan, A. Dubey, H. Knozinger, J. Catal. 231 (2005) 381–392.
[53] G. Fierro, M. Lojacono, M. Inversi, P. Porta, R. Lavecchia, F. Cioci, J. Catal. 148 (1994) 709–721.
[54] A. Alejandre, F. Medina, P. Salagre, X. Correig, J.E. Sueiras, Chem. Mater. 11 (1999) 939.
[55] S. Célerier, S. Morisset, I. Batonneau-Gener, T. Belin, K. Younes, C. Batiot-Dupeyrat, Appl. Catal. A:Gen. 557 (2018) 135–144.
[56] K. Hadjiivanov, G.N. Vayssilov, Adv. Catal. 47 (2002) 307–511.
[57] S. Miyata, Clays Clay Miner. 28 (1980) 50–56.